M

TRAFFIC MANAGEMENT STRATEGIES FOR FREEWAY CORRIDORS PHASE II

2nd EXTENISON

[CONTINUOUS ENHANCEMENTS OF THE KRONOS PROGRAM]

FINAL REPORT

DEPARTMENT OF CIVIL AND MINERAL ENGINEERING
INSTITUTE OF TECHNOLOGY

UNIVERSITY OF MINNESOTA

43533796

TRAFFIC MANAGEMENT STRATEGIES FOR FREEWAY CORRIDORS PHASE II

2nd EXTENISON

[CONTINUOUS ENHANCEMENTS OF THE KRONOS PROGRAM]

FINAL REPORT

JUNE 1991

PREPARED BY

EIL KWON
ROGER PLUM
PANOS MICHALOPOULOS

CENTER FOR TRANSPORTATION STUDIES
DEPARTMENT OF CIVIL AND MINERAL ENGINEERING
UNIVERSITY OF MINNESOTA

TABLE OF CONTENTS

EXECUTIVE SUMMARY

For effective management of freeway systems, it is of critical importance to assess the impacts of various operational strategies before implementation. Developing a reliable traffic simulation program which can test and evaluate "what if" operating policies is an essential element in determining the best management and design scheme to accomodate the traffic demand with available resources.

The University of Minnesota has been developing a microcomputer-based freeway simulation program, KRONOS, under a contract with Mn/DOT for the project entitled "Traffic Management Strategies for Freeway Corridors", which was scheduled to end March 31, 1990. While the prototype version of the program had been completed and proven to have the most appropriate features that Mn/DOT needed, there still remained several problems to be resolved before it could become operational. These included detailed field testing and adjustments of the program with real freeway data, analysis of sensitivities in simulation models with respect to the variations in input data, and enhancements of the input/output module to be suitable for the Mn/DOT planning environment.

The main purpose of this extended project is to make KRONOS operational by resolving the above problems. In addition, a new simulation module to treat merging/diverging of two freeways is developed and incorporated into KRONOS in this project. The major accomplisments made in this extended project are summarized as follows;

- Enhancements of the Input/Ouput module

A new edit function which enables the user to add, delete and replace any freeway segment at any location along the freeway section is developed and added to the input module. This function reduces the time-consuming effort required to prepare different input data files for different geometric types. Further, the new automatic demand loading function developed in this project allows the user to automatically load the demand pattern for each ramp using the ADT

(Average Daily Traffic) data stored in a separate computer file. Other improvements include the input of a flow-density relaitonship, automatic changes to the input demand pattern, etc. In the output module, a new set of performance indices including average flow, density and speed, were added to the Lotus 1-2-3 spread-sheet output file. A new printer module allowing the use of HP printers (Laser and Deskjet) was also developed in this project.

- Enhancements of the intitalization procedure

A new initialization option allows the user to specify the initial state of the freeway section, i.e., congested or uncongested, to be simulated. Further, for consecutive simulaitons over the same freeway section, the last-second results of a previous simulation can be stored and used as the initial condition of a new simulation.

- Development of a new simulation module for merging/diverging of two freeways

A new module to simulate the merging/diverging of two freeways was developed and incorporated into the KRONOS program. The new module was first tested with hypothetical data.

- Processing of the I-35W traffic data

The real traffic data collected from the I-35W freeway in the previous phase of the project was processed and stored in computer files. The final data files contain 5-min. average flow, speed, occupancy and density per lane at the selected locations for 6 peak periods (3-hr/period).

- Analysis of the I-35W traffic data

Using the processed data, a new speed-density relationship was developed for the I-35W freeway. In addition, the speed estimation formula using the volume/occupancy information from the individual detector stations was calibrated for each detector station in the I-35W freeway.

- Validation of the KRONOS program

The KRONOS program was tested and validated with the real traffic data collected from the I-35W freeeway. The test results show very satisfactory model performance with the morning data set where traffic was relatively uncongested (volume: 0.6 - 16%, speed: 2.5 - 28%), while the estimation error increased in two afternoon peak periods in which traffic was heavily congested due to inclimate weather conditions (volume: 7.1 - 28%, speed: 2.8 - 32%).

- Analysis of sensitivities of the simulation models

The sensitivities of the major components in the simulation module, i.e., merging, diyerging and weaving models, with respect to the changes in the input data, including different demand levels and capacity values, were investigated.

I. INTRODUCTION

I.1 Background

The key element in improving freeway operations and performing effective real-time management as well as selecting design plans is the ability to assess the effectiveness of the various alternatives prior to implementation. While simulation methods have long been recognized as the most powerful tool for such analysis, most existing freeway simulation programs are still either in the development stage (1) or lack the sophistication necessary for applications requiring resonably high performance levels (1,2). Furthermore, despite recent advances in microcomputer technologies, the most widely known simulation programs developed to date require main-frame computers (3-6) that are not readily available to most practicing engineers.

To address the above problems, the University of Minnesota had been developing a microcomputer-based freeway simulation program, called KRONOS, under the contract with the Minnesota Department of Transportation (Mn/DOT) for the project entitled "Traffic Management Strategies for Freeway Corridors". While the prototype version of KRONOS had been completed and proven to have the most appropriate features that Mn/DOT needed, there still remained substantial problems to be resolved before it could be fully operational. These problems include detailed field testing of the program and fine-tuning the program's models using data from a real freeway. Another needed improvement was the development of new models to treat freeway segments such as the merging or diverging of two freeways. Further, the KRONOS input/output module features needed to be tailored for the operational environment at Mn/DOT.

To resolve the above problems and to make KRONOS fully operational for Mn/DOT's purposes, the University of Minnesota has been authorized to extend the current project, originally scheduled to end March 31, 1990. This report summarizes the work tasks and the accomplishments of the extended project, the contract for which was signed in July 1990.

I.2 Project objectives

The main objecties of the extended project are to 1) address KRONOS to additional design standards currently in use, and 2) test and validate the KRONOS program using real traffic data. The specific tasks include:

- Development of a new default speed-density curve, or validation of the existing curve, by analyzing the real freeway data collected.
- Testing and validation of the simulation models using the real-world data.
- Analysis of sensitivities in simulation models.
- Operational adjustments of the input/output module.

In addition to the above tasks, a new model to simulate merging/diverging of two freeways was developed and incorporated into the program.

I.3 Report organization

Chapter 2 summarizes the enhancements made to the input/output module and the simulation module. The resulting KRONOS, Version 6.5, provides much more flexibility in terms of data input and output analysis than the previous version. Chapter 3 describes the I-35W traffic data processing results and develops a new speed-density relationship. Further, the speed estimation formula from single-detector data was calibrated for each detector station in the I-35W freeway. Using the processed data, the KRONOS 6.5 is tested and validated in Chapter 4. Finally, Chapter 5 contains conclusions and further research needs.

II. CONTINUOUS ENHANCEMENTS OF THE KRONOS PROGRAM

II.1 Overview of the KRONOS enhancements

The KRONOS program has been continuously enhanced since its inception. Table 1 summarizes the features of each version in chronical order.
The most notable enhancements were incorporated into the KRONOS V6.0. These include substantial reduction of computer execution time through re-organizing the program structure. Further, the input and output procedures were completely revamped and the method of organizing data was revised to take full advantage of single-screen personal computer systems currently available. As a result, it now takes only 12 min. to simulate an 8-mile section of freeway for an hour simulation with the IBM PS/2 (386-25MHZ), while the previous version took 4 hours for the same simulation with the IBM AT computer. In this extended project, the KRONOS V6.0 is further enhanced to be operational in the Mn/DOT planning environment. There are two major directions;

- Improvements of the input/output module to be suitable for a planning environment, such as geometric design, construction and maintenance planning, etc.

- Development of new roadway configuration models for new geometric types, such as the merging and diverging of two freeways, and improvement of existing simulation procedures to improve the accuracy of the simulation results.

Table 1. KRONOS ENHANCEMENTS

Year	Version	Features
1982	1	UCSD-Pascal, 3 types of freeway components, 2-lane/3000 ft. Two monitors required.
1986	4	Microsoft-Pascal, 6 freeway components, 6 lane/10 miles, Two monitors.
1988	5	Microsoft-Pascal, 16 freeway components, Treat Left-Hand-Side ramps, Two monitors.
1990	6	Microsoft-C, 20 freeway components, Treat two lane ent/exit ramps, Single monitor Lotus output interface.

II.1 Enhancements of the Input/Output module

II.1.1 Input module

Major advancements in the modelling process for the input module include:

- Addition of a new edit function for the input of freeway geometric information. The user can now add, delete and replace any freeway segment at any location along the freeway section to be simulated. This enhancement represents a major labor-saving device, especially with respect to exploring different design alternatives.

- Addition of the flow-density curve input function. This function allows the user to enter a flow-density relationship, the data for which is generally much simpler to obtain than for a speed-density relationship. Entering data for the speed-density relationship remains an option. The purpose of this new function is to allow the user to more clearly define the value of critical density, which plays an important role in simulation. Fig.1 illustrates the KRONOS input screen showing the flow-density and speed-density curves.

- Development of an automatic demand data loading function. Using this option, the user can automatically load the demand data for each ramp and for the upstream end of the freeway section by using information, stored in a separate computer file, regarding ADT (average daily traffic volume) and the distribution of ADT over the simulation time period. This function also can significantly reduce the time required to prepare and enter input demand data for KRONOS.

- Automatic increase/decrease of the demand data. This option allows the user to uniformly increase or decrease the existing demand data for each ramp by a certain factor specified by the user. Using this option, various demand patterns (for example uniform growth) can be simulated without re-entering all the demand data.

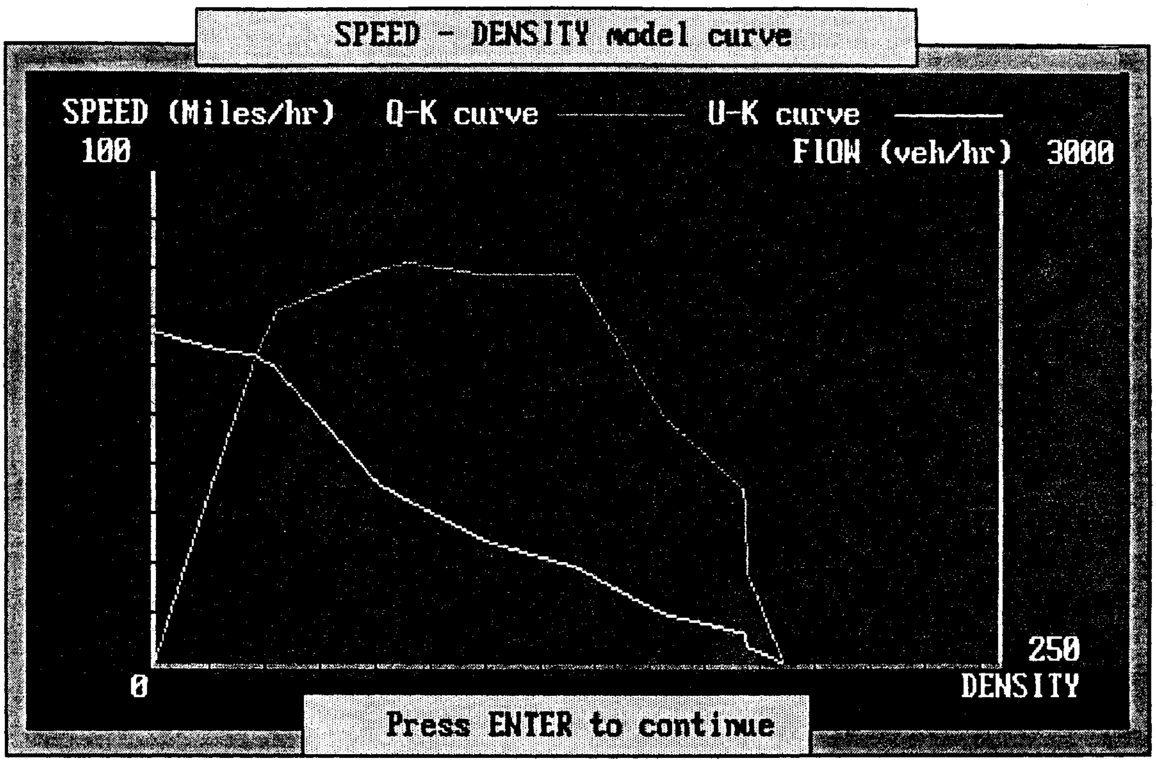

Fig. 1 Input data screen for the speed-density relationahip

In addition to the above enhancements, the new version allows the user to input the demand volume data in different time increments, i.e., volume for 1 to 60 min. (The previous version accepted only an hourly rate.) Further, the new geometric input screen shows the cummulative distance to each segment and the maximum remaining length of the freeway section that can be simulated.

II.1.2 Output module

The major enhancements of the output module include

- New Lotus 1-2-3 spread-sheet format files for average and instantaneous flow, density and speed.

- Addition of a new printer module, which allows the use of Epson (LX, FX, LQ series) and HP (Deskjet, Laser) printers.

II.2 Enhancements of the initialization procedure

The initial condition of the freeway section to be simulated can substantially affect the simulation results, especially when congested traffic conditions are to be simulated. In the previous versions of KRONOS, the initial condition of the entire freeway section is assumed to be uncongested. In this extended project, the initialization procedure was enhanced to allow congested initial conditons on all or selected freeway segments. Further, the arrival demand at the upstream boundary at each time interval can also be specified as congested or uncongested flow. In addition, for consecutive simulations over the same freeway section, the last-second results of the previous simulation can be stored and used as the intial condition of the new simulation. In summary, the new version has the following initialization options;

1) Initialize with the user-specified condition for each segment,
2) Use the previous simulation results,
3) Use the initialization option built into KRONOS.

II.3 Development of new simulation module for merging/diverging of two freeways

In this section, the new algorithm developed for the merging/diverging of two freeways is described with the results of the initial test. Hypothetical freeway data sets are created for the initial testing. The new algorithm is incorporated into the program.

II.3.1 Basic equations in KRONOS

The following equations describe the numerical scheme of KRONOS to estimate the fundamental parameters in traffic, i.e., density, flow and speed, in the descretized freeway section illustrated in Fig.2. These equations form the basis for the detailed modeling of the various traffic movements, such as merging, diverging and weaving, etc. For the detailed background of the basic theory, refer to the KRONOS Final Report, February,1988.

$$K_j(n+1) = \frac{1}{2}(K_{j+1}(n) + K_{j-1}(n)) - \frac{dt}{2dx}(Q_{j+1}(n) - Q_{j-1}(n)) - \frac{dt}{2}(g_{j+1}(n) + g_{j-1}(n)) \qquad \text{(Equation 1)}$$

$$Q_j(n+1) = K_j(n+1) * U_j(n+1) \qquad \text{(Equation 2)}$$

$$U_j(n+1) = U_e(K_j(n+1)) \qquad \text{(Equation 3)}$$

where,

j : index for space coordinate.

n : index for time coordinate.

dx : 100 ft. section of freeway.

dt : simulation interval (1 second).

$K_j(n)$: traffic density at node j in the n-th time step (veh/mile).

$U_j(n)$: traffic speed at node j in the n-th time step (mile/hr).

$Q_j(n)$: flow at node j in the n-th time step (veh/hr).

$U_e(K_j(n))$: the equilibrium speed-density relationship.

$g_j(n)$: the generation term at node j in the n-th time step.

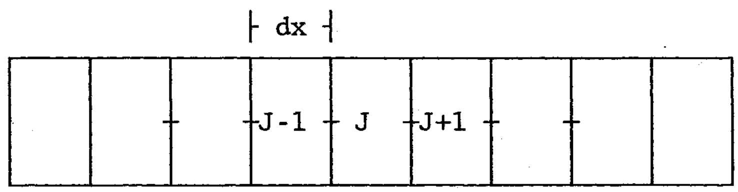

Fig.2 Discretization in space

II.3.2. Modelling of Merging of Two Freeways

This geometric type is new to KRONOS and characterized by two freeways merging together for a short distance and then diverging again, with the number of lanes in the common section being equal to the sum of the number of lanes of the two freeways upstream and downstream of the common section. A typical space discretization of such a section is shown in Fig.3. The system consists of two components, freeways with lane-changing (links B and E) and the remainder (links A, C and D). Links B and E are treated separately, and lane-changing dynamics are considered along the section between links B and link E rather than at a single point.

Modelling of lane-changing is taken into account by the lane- changing term g(x,t) in the numercial solution of the conservation equation (Eq. 1). Lane changing dynamics are considered not only explicitly at the boundaries of links B and E but also implicitly between lanes on each link. When average lane flow between links B and E are unbalanced, the traffic on the heavier link tends to change to another link for better driving conditions and this flow represents the lane-changing term between two links. This lane-changing term is averaged and spreads over all the lanes on each link.

The following numerical algorithm allows computation of density (K), speed (U) and flow (Q) at each node of the discretized freeway system.

(A) Links A, C and D

These links are characterized by the absence of flow generation. Density, speed and flow at the internal nodes 1 to J_p(p = { A, C, D }) are given by Equations 1, 2 and 3. If O_A is the first node of the simulation section then it is treated as an external boundary where the boundary condition of $K_{OA}(n+1)$ and $U_{OA}(n+1)$ is determined from the input demand pattern. From known $Q_{OA}(n+1)$, the corresponding density and speed are determined. Otherwise, the values are derived from Equations 1, 2 and 3. If node J_C is the downstream boundary of simulation section, then it is treated as an external boundary. Node O_D is the

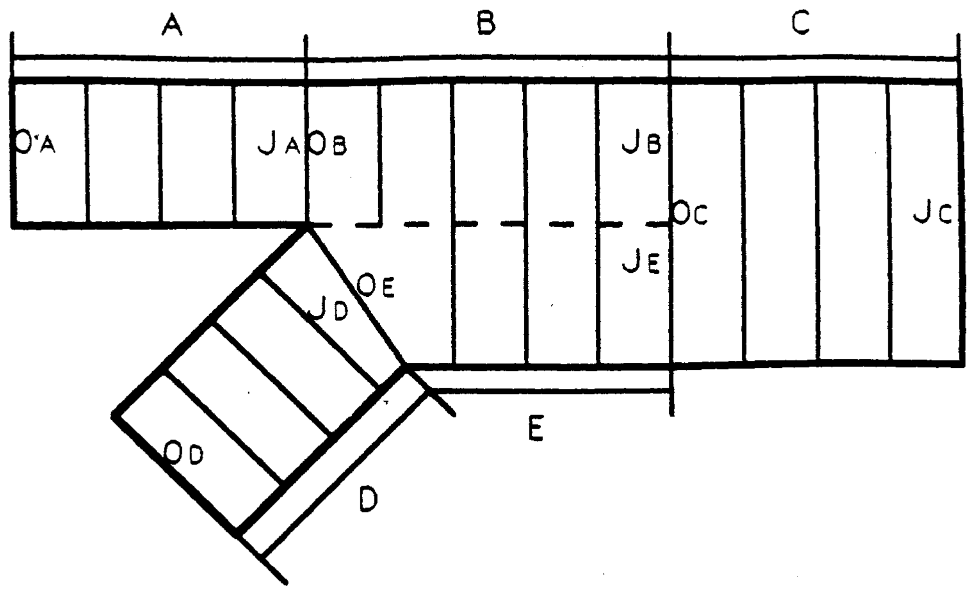

Fig. 3 Space discretization of a typical merging segment

upstream boundary of the merging freeway. Thus, $K_{OD}(n+1)$ and $U_{OD}(n+1)$ are determined from the demand pattern.

(B) Links B and E

These links are characterized by the fact that lane-changing may occur between two links. Lane-changing between links B and E is treated explicitly and is assumed to occur along the entire section (as opposed to at a single point within the section). Specifically:

Step 1: Determine lane-changing demand at each node j over link B and E by comparing the average lane flow of link E with that of link B

$$q_{j,1}(n) = ((Q_{j,B}(n)*NL_B+Q_{j,E}(n)*NL_E)/(NL_B+NL_E)-Q_{j,B}(n))*NL_B$$

where,

$Q_{j,B}(n)$, $Q_{j,E}(n)$ = average lane flow at node j of link B and E in the n-th time step

$q_{j,1}(n)$ = lane-changing demand at node j in the n-th time step

NL_B, NL_E = number of lanes on links B and E

Step 2: Determine the generation term at each node of link B and link E:

if $q_{j,1}(n) > 0$ (average lane flow at node j of link E is greater than that of link B, lane-changing occurs from link E to link B);

otherwise $q_{j,1}(n) < 0$ (average lane flow at node j of link E is less than that of link B, lane-changing occurs from link B to link E).

Calculate generation term from:

$$g_{j,E}(n) = \frac{q_{j,1}(n)}{dx} \frac{1}{(J_E - j + 1)}$$

$$g_{j,B}(n) = - g_{j,E}(n)$$

where,

$g_{j,E}(n)$ = generation term at node j of link E in the n-th time step

$g_{j,B}(n)$ = generation term at node j of link B in the n-th time step

J_E = the last node of link E (it is assumed that $g_{j,E}(n)$ decreases linearly with distance)

Step 3: With the generation term known, calculate K and corresponding U and Q for the link B and for the link E separately from Eqs. (1), (2) and (3). At each node of links B and E, the generation term is added/subtracted and averaged across all the lanes in each link.

II.3.3 Testing of the freeway merging model

Hypothetical geometrics and demand patterns are used for the initial testing. Fig.4 shows the hypothetical geometrics of the merging of two freeways, where a two-lane freeway is merged into another two-lane freeway and continues as a four-lane freeway without the loss of a lane. Demands of two freeways were changed in every odd-numbered time slice to keep the demand sum of two freeways constant (6000 vph).

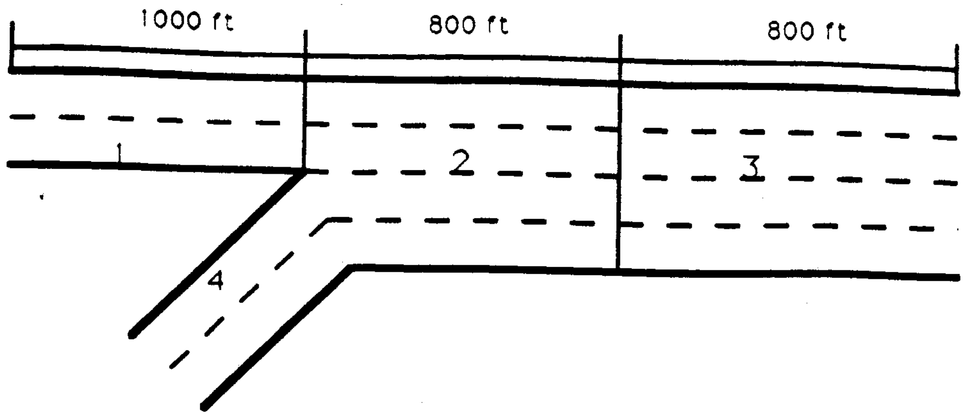

a. Geometrics

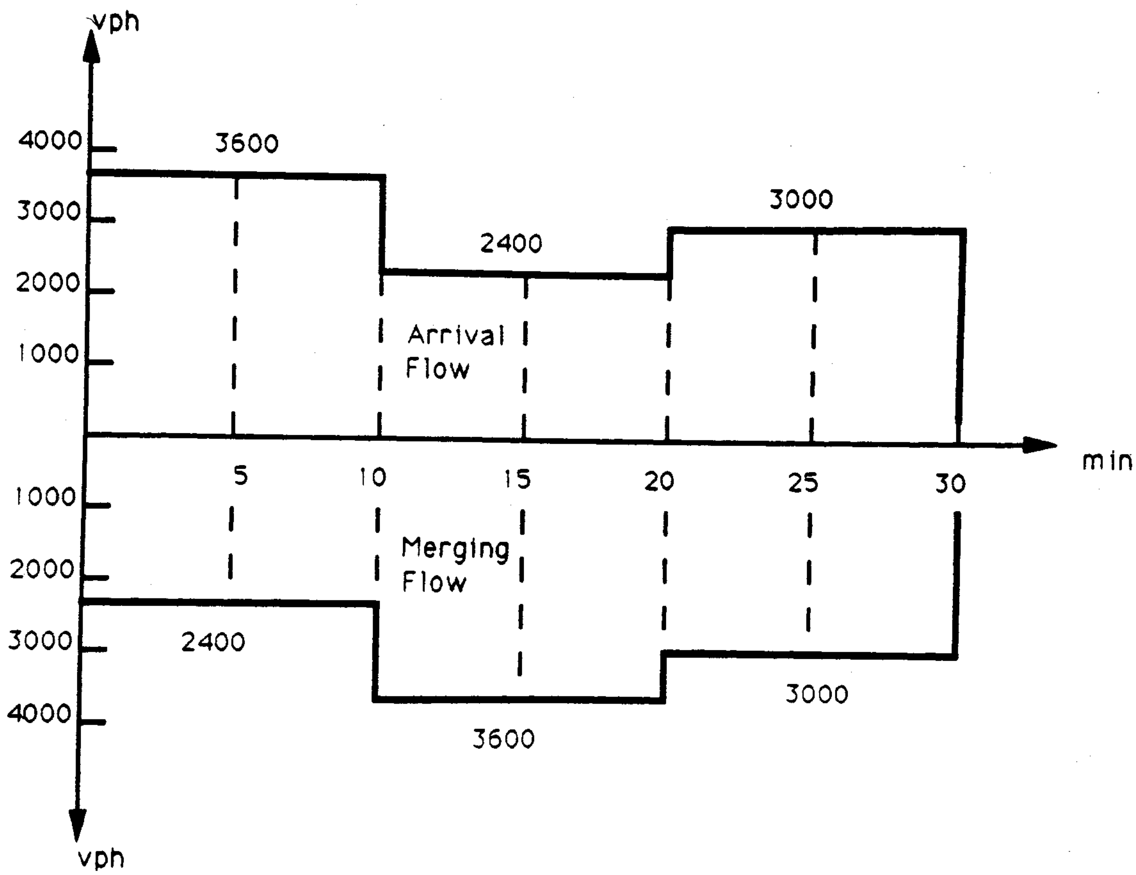

b. Demand Pattern

Fig. 4 Geometrics and Demand Pattern of the example merging area

The results of testing are presented in Table 2, where 30-minute simulation results are summarized for six time slices. Zone four represents the freeway merging section. The number of vehicles passing the end of each zone during each time slice is a measure of the accuracy of the modelling. The capacity of every section being greater than the demand implies uncongested operation during the simulation; therefore, the number of vehicles passing the end of zone 3 (after merging) during the even-numbered time slices should be the demand sum of zones 1 and 4, which was constant (6000 vph).

Implementation of the modelling of the section including the merging of two freeways revealed satisfactory results in terms of the conservation of the volumes at the end of each zone. Table 2 shows that the number of vehicles passing the end of zone 3 during even-numbered time slices are close to 500 veh/5 min (6000 vph). We can also see the expected speed distributions for zones 2 and 3, which remained constant over all time slices.

Table 2. Testing of a Merging of Two Freeways (Hypothetical Situation)

Time Slice		Zone 1	Zone 2	Zone 3	Zone 4
1 (5 min)	Vol[1)] :	283	500	500	200
	Speed[2)] :	47.7	50.7	50.7	51.2
2 (10 min)	Vol :	283	499	499	200
	Speed :	47.7	50.7	50.7	51.2
3 (15 min)	Vol :	213	502	502	300
	Speed :	51.1	50.7	50.7	48.0
4 (20 min)	Vol :	209	500	500	300
	Speed :	51.2	50.7	50.7	47.9
5 (25 min)	Vol :	251	504	504	250
	Speed :	50.7	50.7	50.7	50.7
6 (30 min)	Vol :	252	505	505	250
	Speed :	50.7	50.7	50.7	50.7

1) Vol : number of cars passed at the end of each zone during each time slice (5 minutes)

2) Speed: Space mean speed (mph) for each zone during each time slice

II.3.4 Modelling of Diverging of a Freeway into Two Freeways

This geometric type is also new to KRONOS and characterized as the diversion of a freeway, in which the total number of lanes before and after the diversion is conserved.

A typical space discretization of such a section is shown in Fig. 5. The system consists of two components, freeways with lane-changing (links B and D) and the remainder (links A, C and E). Links B and D are treated separately and lane changing dynamics are considered implicitly at a single point.

The following numerical algorithm allows computation of density (K), speed (U) and flow (Q) at each node of the discretized freeway system.

(A) Links A, C and E

These links are characterized by the absence of flow generation. Density, speed and flow at internal nodes 1 to J_p(p = { A, C and E }) are given by Eqs. (1), (2) and (3). If node 0_A is the beginning of the simulation section, it is treated as an external boundary where the boundary condition is given by the demand pattern. Otherwise, the values are determined from Eqs. (1), (2) and (3). If node J_C is the downstream boundary of the simulation section, it is treated as an external boundary. Node J_E is the last node of the diverging freeway and treated as an external boundary.

(B) Links B and D

These links represent the section where lane-changing movements may occur. Lane-changing between links B and D is treated implicitly and is assumed to occur at the first node. Lane-changing cannot be considered explicitly because diverging demand is dynamically changing. Specifically:

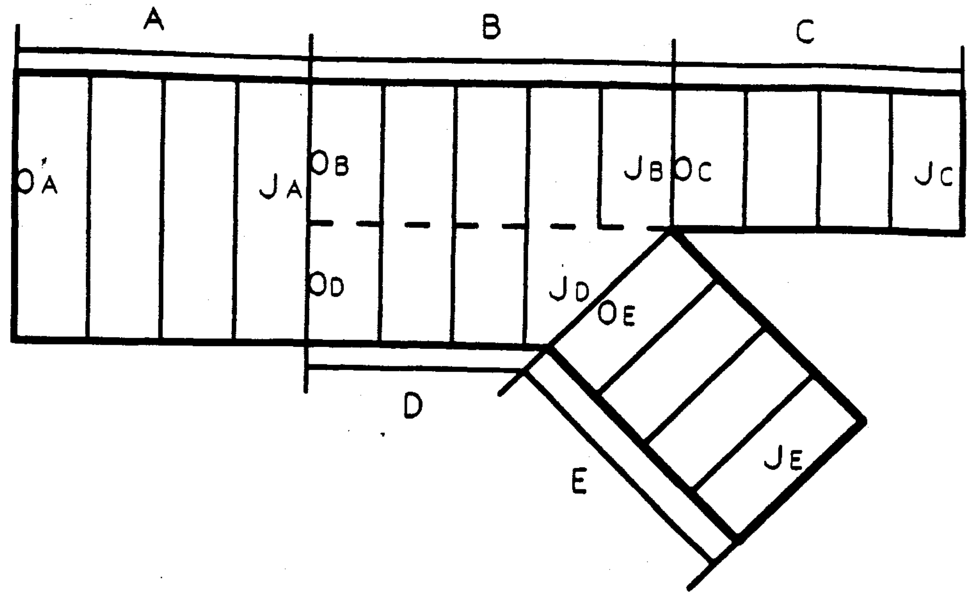

Fig. 5 Space discretization of a typical diverging segment

Step 1: Diverging demand of volume $Q_{div}[J_A,n]$ in each time slice is specified by the input

Step 2: From the diverging demand $Q_{div}[J_A,n]$ get the corresponding speed and density and set to boundary values of O_D. If the flow condition at node O_D+1 is congested, get density and speed from congested region of Q-K curve, otherwise, obtain it from uncongested region. Speed, density and flow on links D and E are calculated from eqns (3-1), (3-2) and (3-3). Node $J_D(O_E)$ is not treated as a boundary.

Step 3: Get the lane-changing term from the following equation:

$$q_l[J_A,n] = Q_{JA}(n)*lane[D] - Q_{div}[J_A,n]$$

where, $q_l[J_A,n]$ = lane-changing demand at node J_A in the n-th time step

$Q_{JA}(n)$ = average lane flow at the last node of link A in the n-th time step

lane[D] = number of lanes on link D

$Q_{div}[J_A,n]$ = diverging demand at node J_A in the n-th time step

Step 4: With the lane-changing term known, set the boundary condition at the node O_B of link B:

$$Q_{OB}(n) = Q_{JA}(n) + q_1[J_A, n]/NL_B$$

where, $Q_{OB}(n)$ = average lane flow at the last node of link A in the n-th time step

NL_B = number of lanes on link B

Step 5: From the known flow $Q_{OB}(n)$ get the corresponding density and speed and set the boundary condition. If the flow condition at node O_B+1 is congested get density and speed from congested region of Q-K curve, otherwise obtain it from uncongested region. Speed, density and flow of links B and C are calculated from Eqns. (1), (2) and (3). Node $J_B(O_C)$ is not treated as a boundary.

III.3.5 Testing of the diverging model

Fig. 6 shows the hypothetical geometrics created for testing purposes, where a four-lane freeway diverges into two 2-lane freeways. Demands upstream of the freeway in each time slice are kept constant, and the demand of the diverging freeways are changed in every odd-numbered time slice. Table 3 shows the 30-minute simulation results, where the duration of each time slice is 5 minutes. Zone 4 represents the diverging freeway section. The number of vehicles counted at the end of each zone is a measure of the accuracy of the modelling. Because the capacity of every section is greater than the demand, the sum of the cars passing the ends of zones 3 and 4 (diverged freeways) during

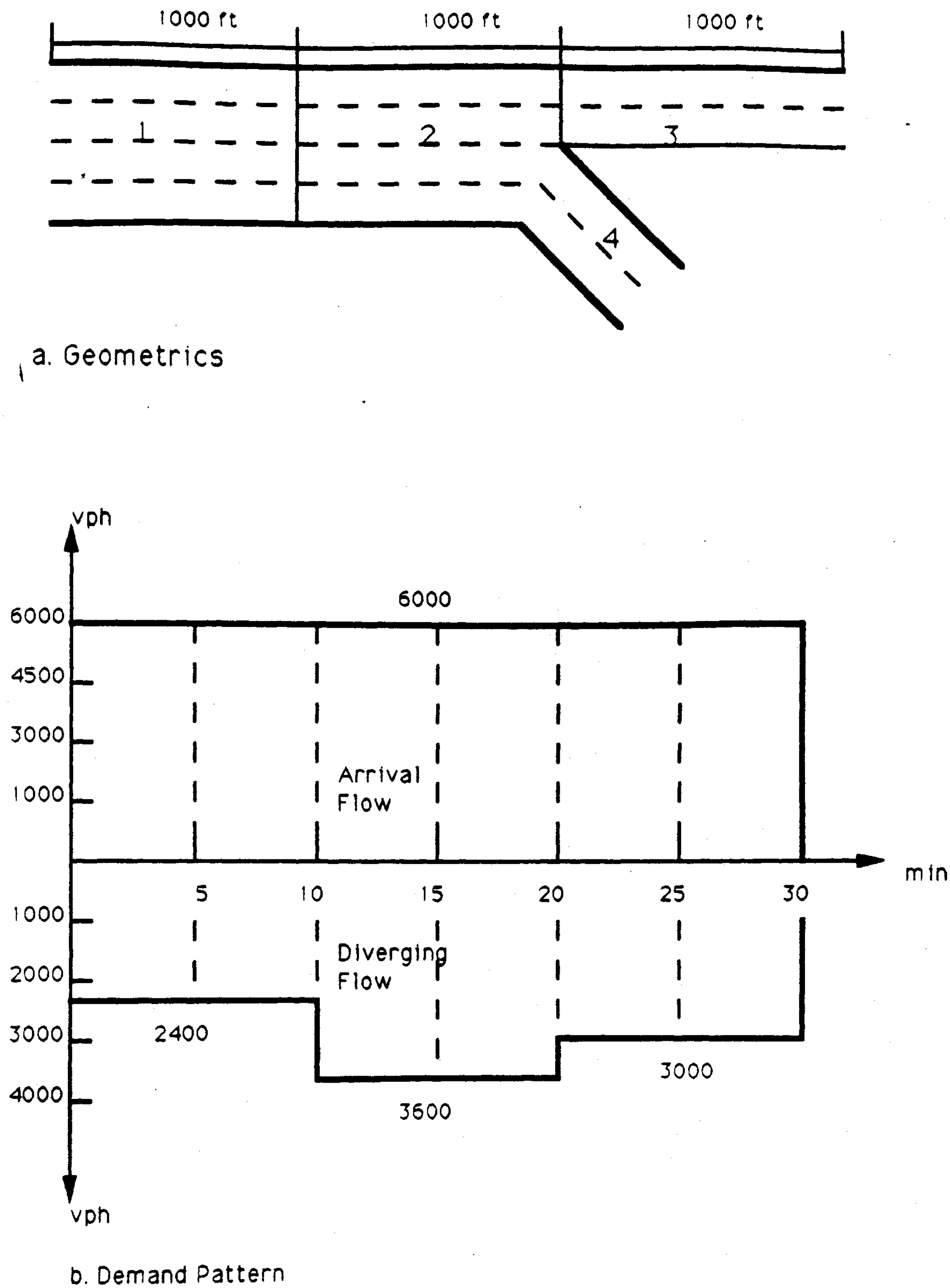

Fig. 6 Geometrics and demand pattern of the example diverging area

the even-numbered time slices should be equal to the upstream demand, which was constant (6000 vph).

Error indices less than 1.0 % indicate close agreement of the proposed modelling in terms of the conservation of the volumes. Table 3 shows that the number of vehicles passing the end of zones 3 and 4 during even time slices are close to 500 veh/5 min (6000 vph).

Table 3. Test results of the diverging model with the example data (Hypothetical Situation)

Time Slice		Zone 1	Zone 2	Zone 3	Zone 4	$Error_{3)}$
1 (5 min)	$Vol_{1)}$:	509	501	297	203	
	$Speed_{2)}$:	50.7	47.8	46.9	51.2	
2 (10 min)	Vol :	509	502	301	201	-0.4
	Speed :	50.7	47.6	46.4	51.2	
3 (15 min)	Vol :	510	506	221	285	
	Speed :	50.7	50.2	50.6	47.8	
4 (20 min)	Vol :	510	506	211	295	-1.2
	Speed :	50.7	50.2	51.1	47.4	
5 (25 min)	Vol :	511	516	256	257	
	Speed :	50.7	50.3	50.2	50.4	
6 (30 min)	Vol :	511	515	253	252	-1.0
	Speed :	50.7	50.3	50.2	50.7	

1) Vol : number of cars passed at the end of each zone during every time slice (5 minutes)

2) Speed: Space mean speed (mph) for each zone during each time slice

3) $$\text{Error} = \frac{\text{Demand} - (\text{Vol(Zone 3)} + \text{Vol(Zone 4)}}{\text{Demand}} * 100\ (\%)$$

III. I-35W TRAFFIC DATA PROCESSING

III.1 Overview of the I-35W traffic data

To test and calibrate the KRONOS simulation models in the Twin Cities traffic environment, real speed-volume data were collected from an 8-mile section of the I-35W freeway in the previous phase of this project (7). Since the current Mn/DOT loop detection system provides only volume and occupancy measurements, the speed data were collected manually using stopwatches. Fig.7 illustrates the data collection sites, which coincides with locations where loop detectors already exist. A total of 70 people were hired on a temporary basis and trained to cover 35 collection sites for 6 peak periods on 6 different days in November 1989. The following data were collected;

1) Approximately 6500 data sheets containing sample travel time measurements of vehicles passing between two observation posts for each lane, for every 5-min. interval,

2) 6 loop detector files including the measurements of volume/occupancy passing the observation posts on the mainline and merging/exiting volume at ramps every 5-min. interval,

3) 18 tube detector files covering ramps where loop detectors malfunctioned.

4) Heavy commercial vehicle counts at selected locations.

The rest of this chapter describes the processing procedure and the analysis results of the above data.

I35W TRAFFIC MONITERING SITES

OFFICE OF FREEWAY OPERATIONS & THE UNIVERSITY OF MINNESOTA

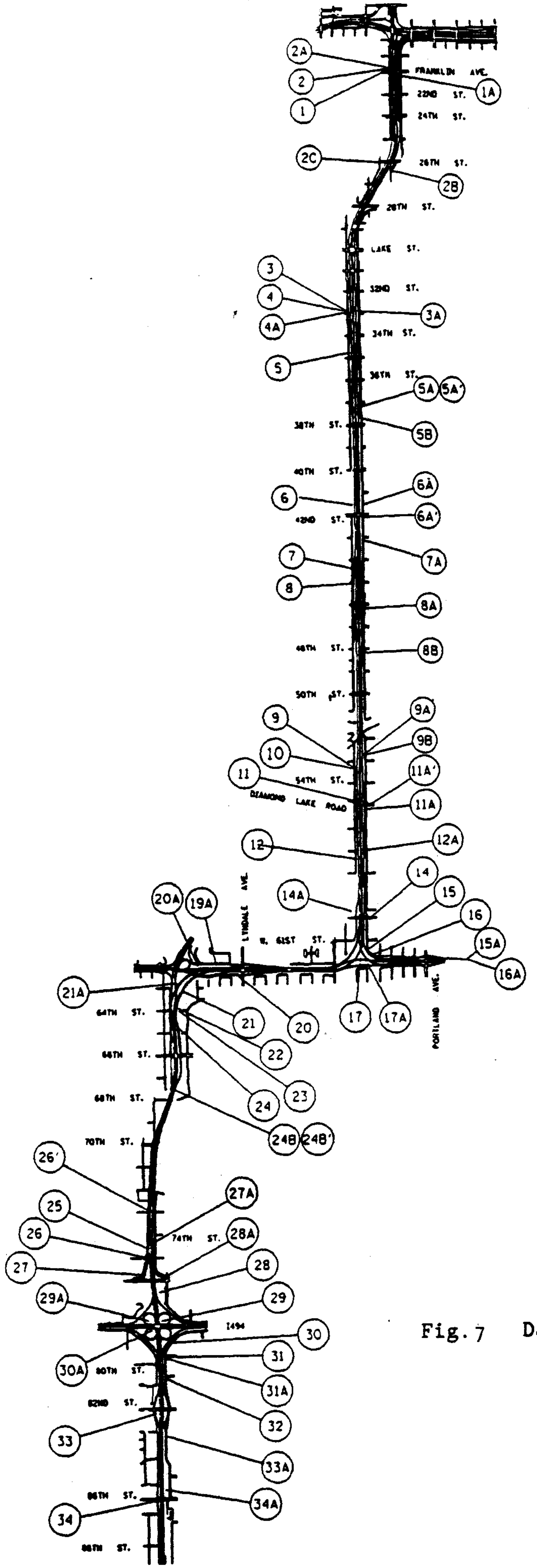

Fig. 7 Data collection sites in the I-35W freeway section

III.2 Data coding and processing

First, the travel time measurements recorded in the data sheets were coded into computer files. Each travel-time data file contains one-day measurements for one site. A total of 174 files were produced by Mn/DOT (157 files) and by the U of Mn (15 files) with two different types of format, i.e., ASCII and Lotus. These data files were converted to have a common format suitable for the statistical treatment, which eliminated measurement errors and calculated average speed values. A comprehensive data processing program was developed to treat data statistically and to combine the resulting speed information with other data, such as volume and occupancy. The processing program graphically displays the travel-time measuements for each lane on the computer screen for the visual detection of outliers. After eliminating outliers, the program produces speed, volume and occupancy data for every 5 min. interval by combining volume and occupancy information stored in other files. The final data structure consists of 6 files, one for each day, in Lotus spread-sheet format. Fig.8 illustrates the data processing procedure adopted in this project.

III.3 Development of the new speed-density relationship

Using the speed-flow data processed as described in the previous section, a speed-density relationship was derived for the I-35W test freeway section. Fig.9 - 10 shows the speed(flow)-density plots derived from measurements for 4 peak periods. In this research, all 6 days' measurements were used to derive a single, representative speed-density relationship for the I-35W freeway. The resulting curve and data points are shown in Fig.11. However, it should be noted that, depending on traffic conditions, such as weather and geometrics, there could be significant variations in the speed-density relationships for the same roadway section. For example, Fig.9 shows the speed(flow)-density

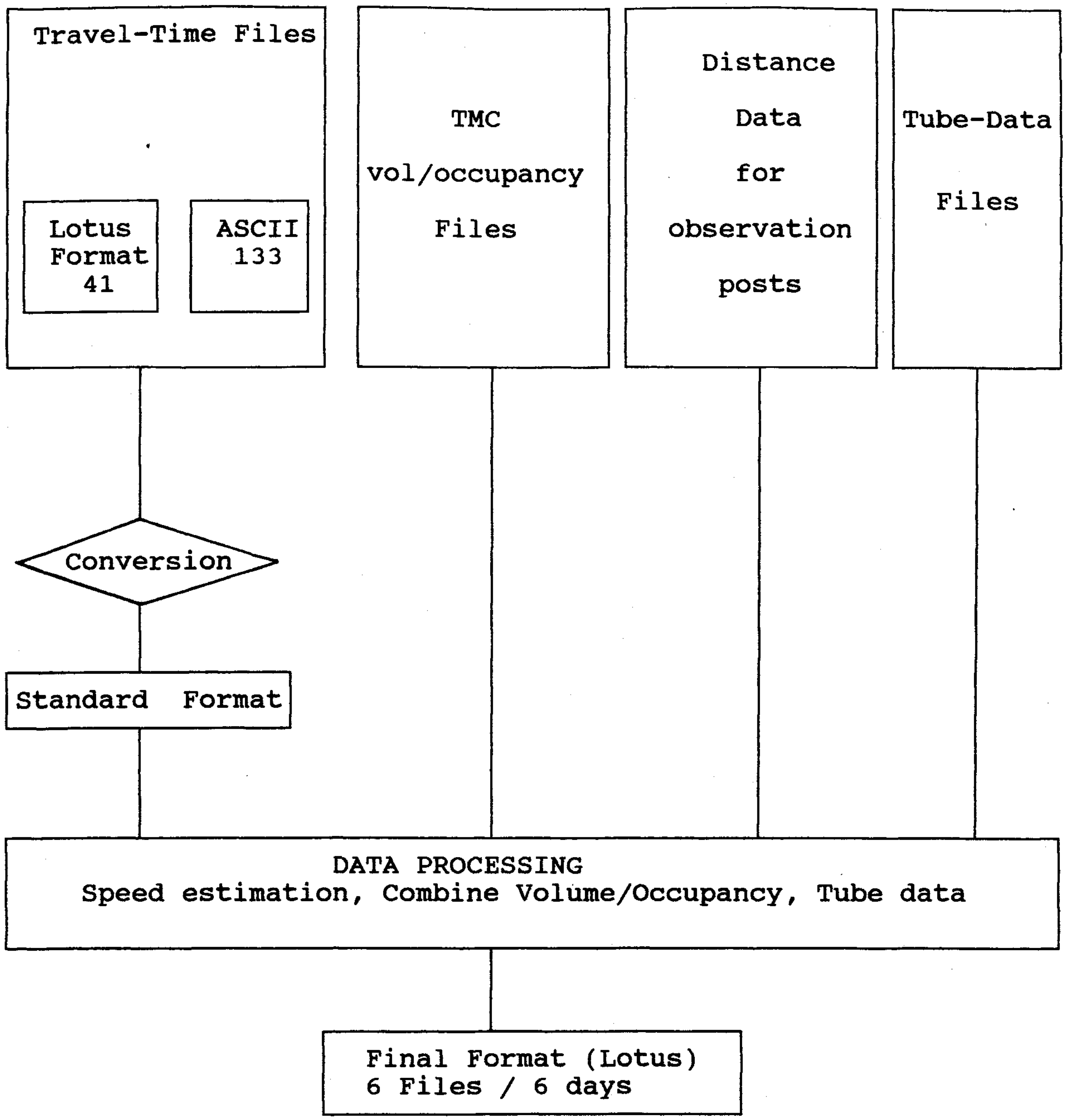

Fig. 8 Data processing procedure

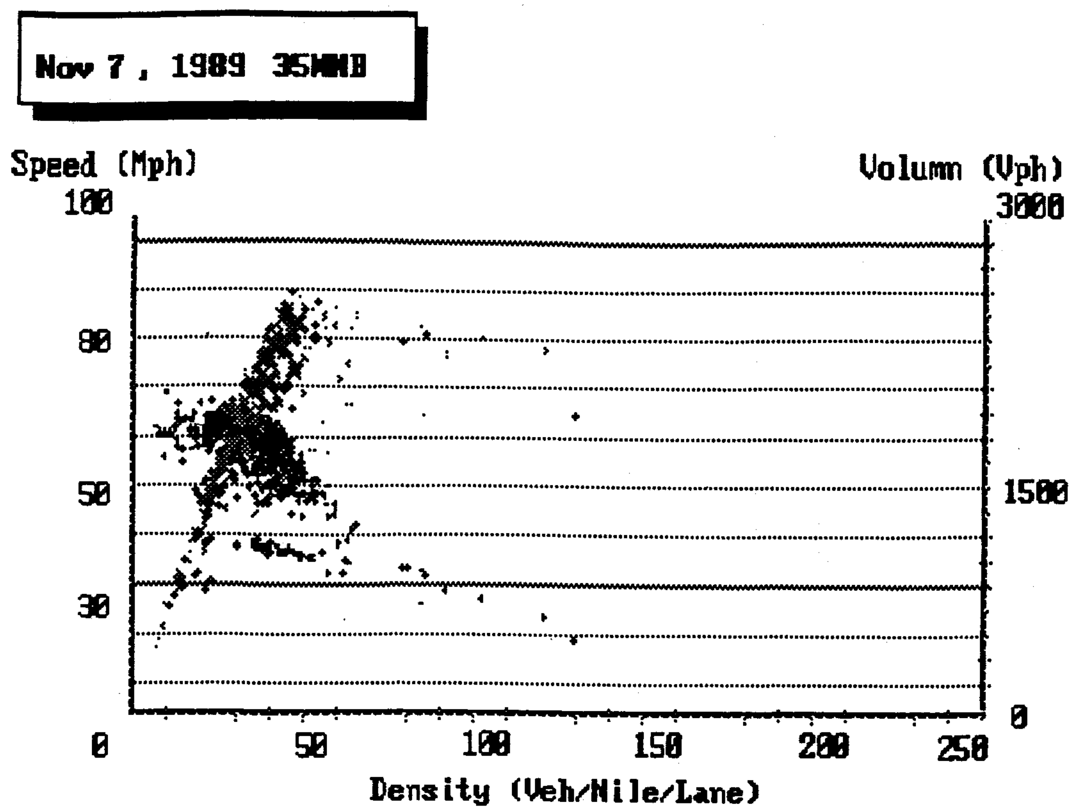

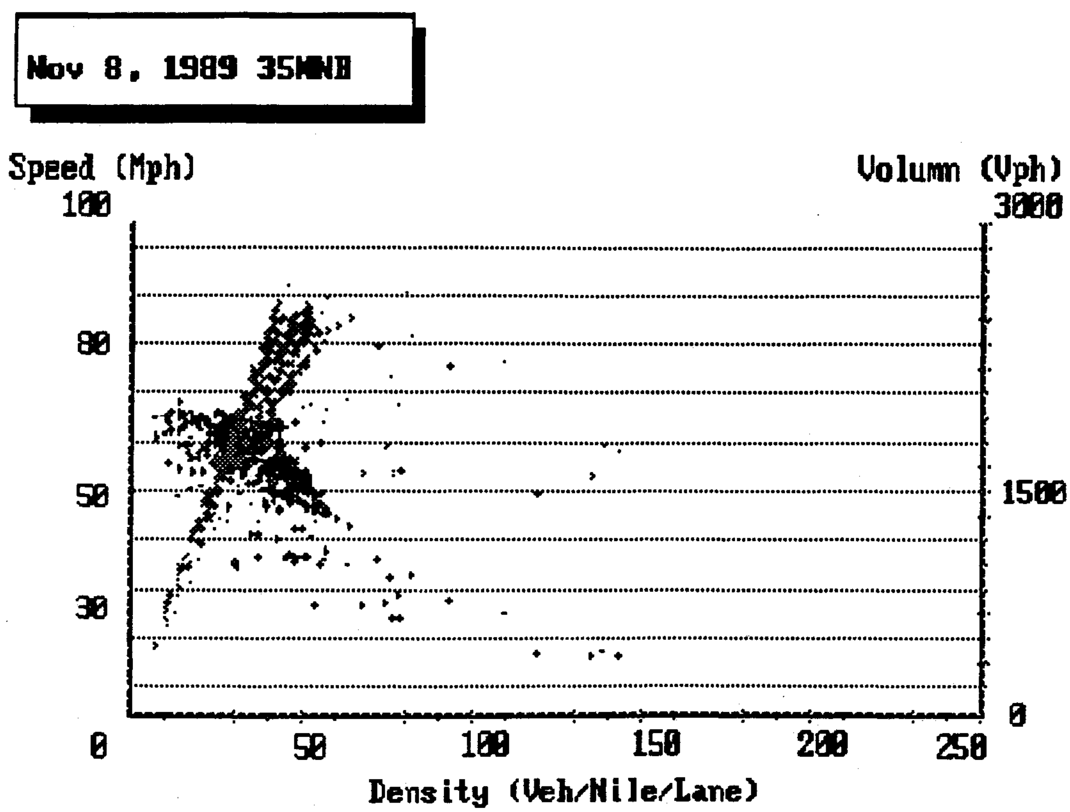

Fig. 9 Speed (flow) - density relationship (I-35W North Bound, Morning)

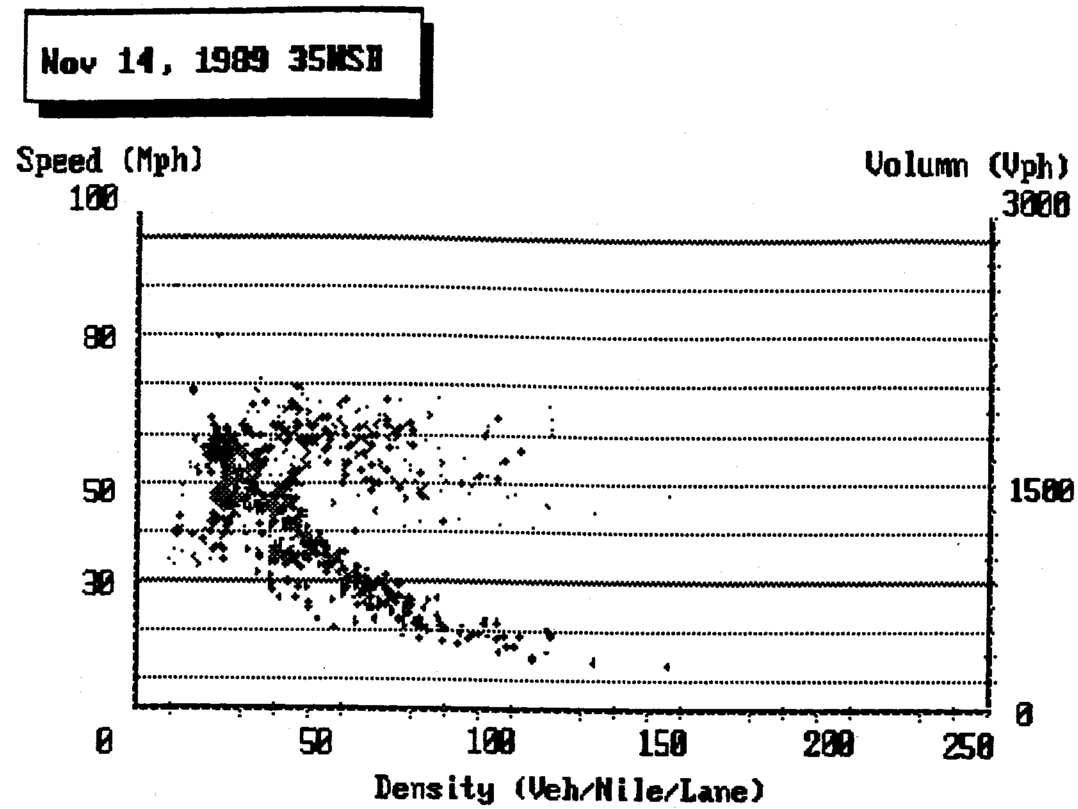

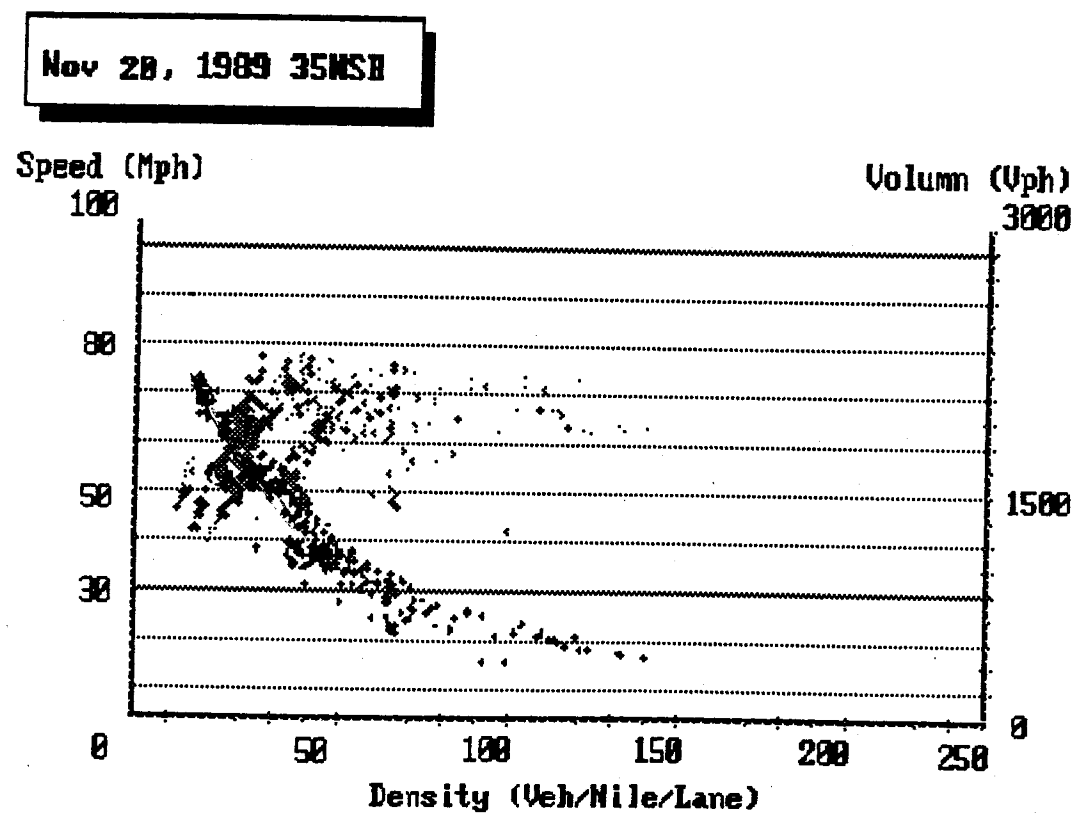

Fig. 10 Speed (flow) - density relationship (I-35W South Bound, Afternoon)

Points	Density (veh/mile)	Speed (miles/hr)	Flow (veh/hr)
1	0.00	67.00	0.00
2	10.00	65.00	650.00
3	20.00	63.00	1260.00
4	30.00	62.00	1860.00
5	32.00	61.00	1952.00
6	35.00	60.00	2100.00
7	36.00	59.00	2124.00
8	66.00	36.00	2376.00
9	76.00	32.00	2432.00
10	98.00	24.00	2352.00
11	124.00	19.00	2356.00
12	150.00	10.00	1500.00
13	174.00	6.00	1044.00
14	175.00	3.00	525.00
15	186.00	0.00	0.00

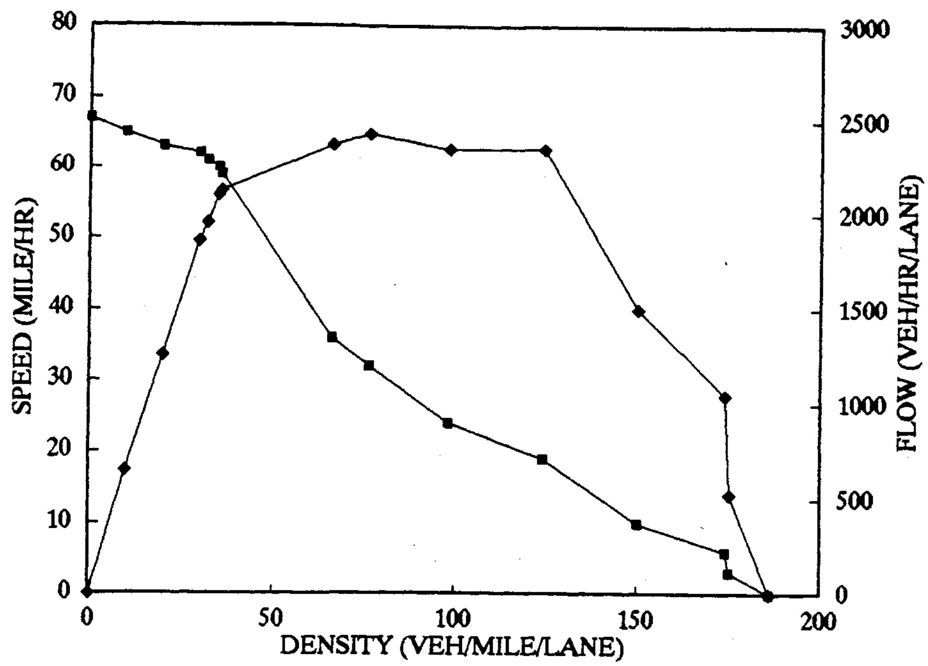

Fig. 11 A new default speed(flow)-density relationship

relationships for the morning traffic in the north bound I-35W freeway section, while Fig.10 shows the same relationships for the afternoon, south bound I-35W traffic with inclimate weather conditions. Further, Fig.12 illustrates the speed-density relationships at two locations with different lane configurations, i.e., 2-lane vs 3-lane. As shown in these figures, the speed-density relationships can vary significantly depending on locations and weather conditions, which illustrates the limitations in using a single speed-density relationship for the entire freeway section.

III.4 Calibration of speed estimation parameters for single-detector stations

Speed information plays an important role in traffic management as a potential indicator of problems on the roadway and a good measure of system effectiveness. While speed data can be directly measured by using closely spaced pairs of detectors, which can calculate speeds on the basis of the time taken to cross the gap between the detectors, the current Mn/DOT detection system consists of the single-detector stations which provide only volume and occupancy measurements. In this section, the speed estimation procedure from single-detector data, i.e., volume and occupancy, is calibrated by using the I-35W data processed in the previous section. The following formula is generally used to calculate speed in the absence of pairs of closely spaced detectors.

$$\text{speed} = \alpha \text{ (flow/occupancy)}$$

where α is a constant to convert the units to their proper values and is related to mean vehicle length plus detector size. While the above formula is based on assumptions that are not valid in case of extreme traffic conditions, i.e., very light and heavy, it provides reasonable estimates of speed for most of the range of uncongested traffic (roughly 8 to the mid-20 % range of occupancies) (8). In this section, the value of α in the above formula is calibrated by using the

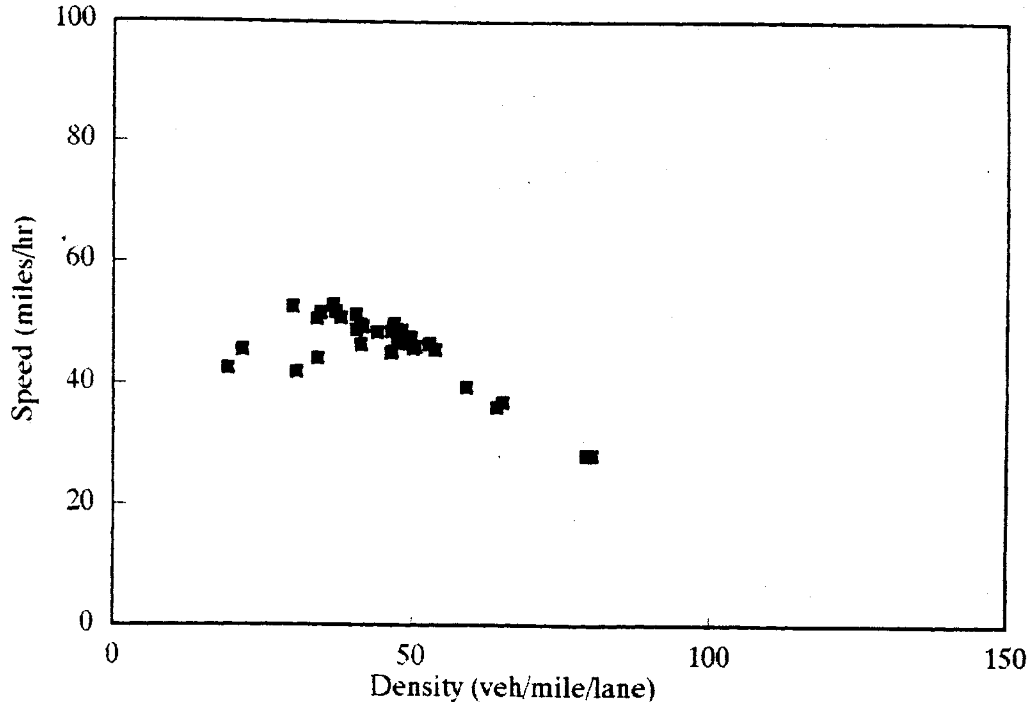

Location: I−35W nb 53N (3 lanes)
Date: Nov. 7, 1989

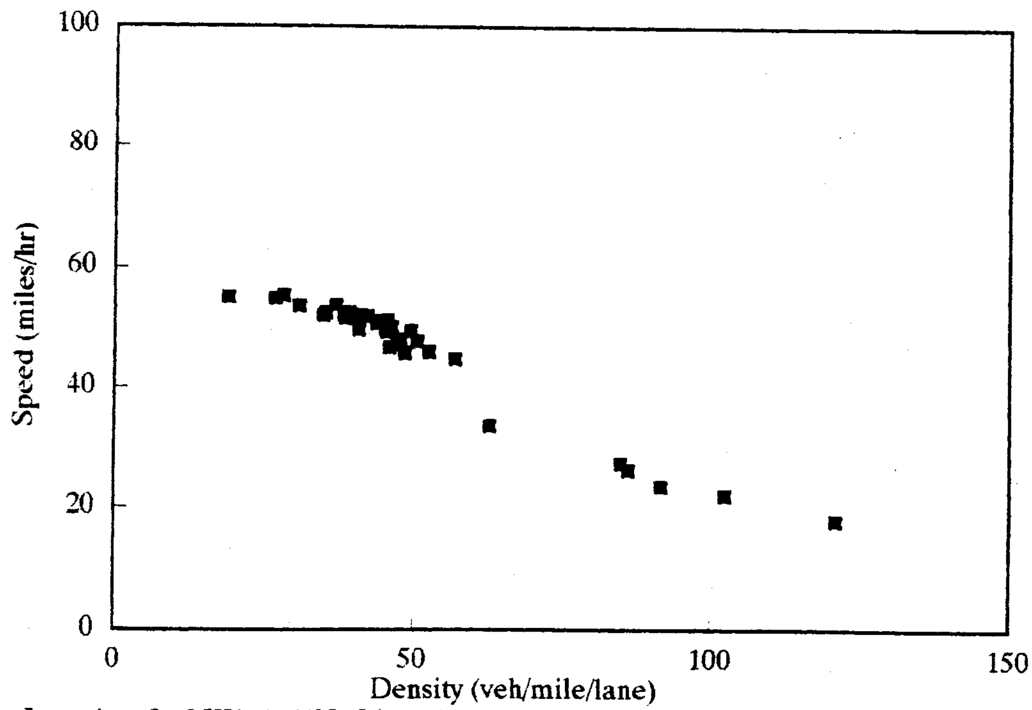

Location: I−35W nb 61N (2 lanes)
Date: Nov. 7, 1989

Fig. 12 Speed-density relationships at different geometrics linear regression technique for each detector station where the speed data was collected along with volume and occupancy data. The 5-min. volume and 5-min. occupancy data were used in this calibration, i.e.,

$$\text{Speed (mile/hr)} = \alpha \text{ (5-min. Volume)/(5-min. Occupancy)}$$

Tables 3 and 4 shows the resulting α values for each station . The t-statistics indicate that all α values are statistically significant at the 95% confidence level.

From Table 3 and 4, it can be seen that there are significant variations in α values across the stations, while small variations exist at the same detector stations over different days. The fact that different locations have different α values seems to indicate that there exist substantial variations in terms of the sensitivity ranges in loop detector stations.

Table 3. Calibration results (I-35W North Bound)

(t-statistics)

LOCATION	11/7	11/8	11/9	
86N	4.98 (78.7)		4.99 (151.2)	4.98 (192.3)
82N	5.31 (108.4)	5.46 (91.03)	5.37 (92.0)	
78N				
76N	5.27 (142.5)	5.12 (74.9)	5.20 (123.5)	
73N			5.24 (84.1)	
70N	4.98 (78.7)	5.34 (78.1)	4.43 (149.7)	
66N				
63N				
62N				
61N	4.74 (79.2)	4.93 (144.5)	4.83 (136.1)	
60N	5.52 (50.7)	5.44 (56.9)	5.30 (60.2)	
55N	4.68 (117.2)	3.89 (125.3)	4.62 (98.5)	
53N	4.31 (99.3)		4.57 (44.8)	
50N				
46N				
42N				
38N				
35N	3.89 (176.4)		3.83 (144.2)	
31N				
28N				
26N	4.97 (95.0)		4.70 (141.0)	
20NX				
20N	4.50 (89.0)		4.64 (95.6)	

Table 4. Calibration results (I-35W South Bound)

(t-statistics)

LOCATION	11/14	11/20	11/21	
86S				
82S				
78S				
76S	5.18 (61.8)	5.13 (109.3)	5.98 (16.7)	
73S				
70S	2.78 (112.9)	2.73 (151.4)	2.13 (8.3)	
66S				
63S	4.49 (64.9)	4.54 (102.9)	4.64 (20.0)	
62S	6.50 (32.1)	19.2 (67.6)	15.1 (34.1)	
61S	3.00 (23.0)	5.57 (62.5)	5.46 (66.4)	
60S	4.37 (39.3)	4.71 (78.4)	3.11 (60.1)	
55S				
53S		4.71 (46.9)		
50S	4.45 (37.0)	3.90 (50.1)		
46S	3.62 (12.9)	3.13 (49.4)		
42S		4.75 (35.1)	7.00 (26.2)	
38S				
35S	4.31 (28.8)			
31S				
28S				
26S				
20Sm	5.50 (93.0)	6.22 (53.7)	5.62 (96.7)	
20S	4.30 (94.9)	4.28 (82.6)	4.23 (47.6)	

IV. TESTING AND VALIDATION OF THE KRONOS PROGRAM

IV.1 Test sites and input data preparation

The enhanced KRONOS, V6.5, is tested and validated using the I-35W freeway section, where the traffic data were collected, as the test section. Fig.13 & 14 illustrate the schematic representation of the 8-mile test section in both directions. While the collected data contains 6 days' measurements for the test section, due to detector malfunctions, only 4 days' data were usable to create 3 hours of consecutive input volume information for all ramps in the test section. Using the real-volume data collected from the upstream boundary and entrance/exit ramps as the demand pattern for the test freeway section, 4 input data files for the KRONOS simulation were prepared. The capacity of each individual freeway segment was estimated by using the Highway Capacity Manual and field observations.

IV.2 Validation results

The 8-mile test freeway section was simulated with the new speed-density relationship, developed in the previous chapter, for 4 days, i.e., 2 morning and 2 afternoon peak periods. The simulation results were compared with the real volume/speed data collected from the test section.

To evaluate quantitatively the model performance, the following error measurements are calculated:

Percentage Difference (PD: %): $100 * (\text{Measured} - \text{Estimated})_k \,/\, \text{Measured}_k$

Mean Percentage Difference (MPD: %):

$$\sum \left[\ 100 * (\text{Measured} - \text{Estimated})_k \,/\, \text{Measured}_k\ \right] / N$$

Mean Absolute Error (MAE):

$$\sum \left[(\text{Measured} - \text{Estimated})_k\right] / N$$

where N = the number of measured points.

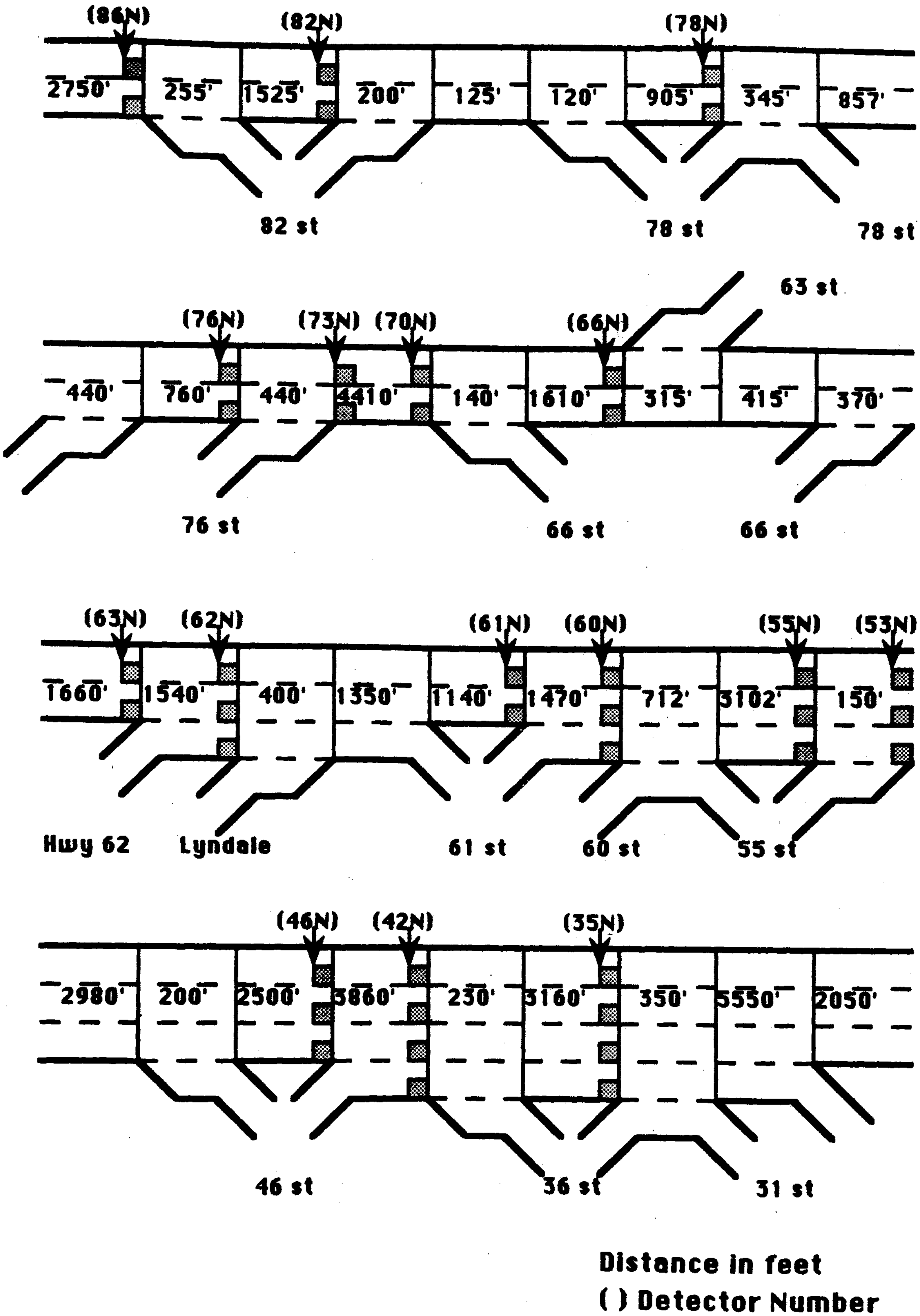

Fig. 13 Geometrics of the test section (I-35W, Northbound)

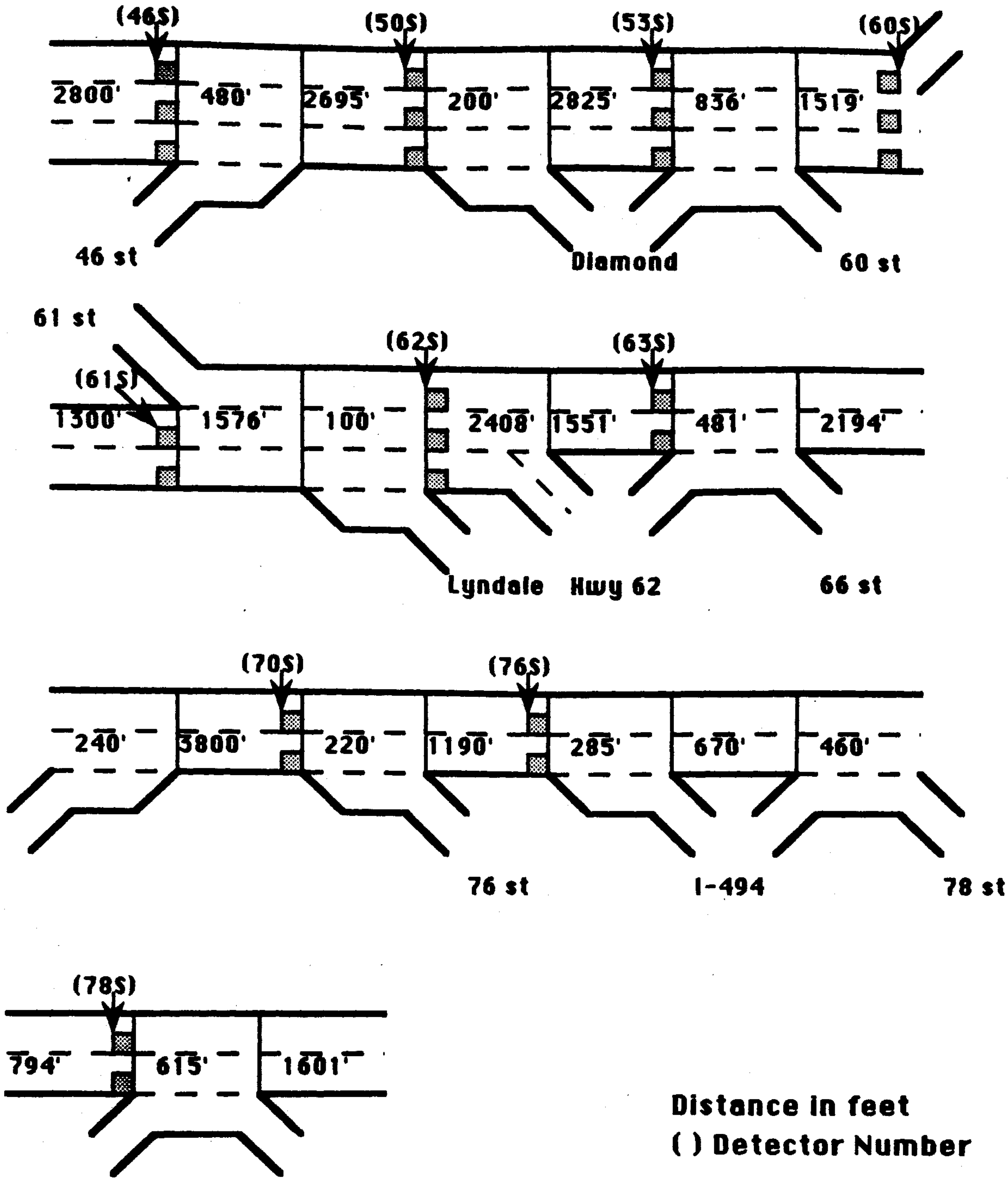

Fig. 14 Geometrics of the test section (I-35W, Southbound)

Figures 15 - 16 illustrate the error (Percentage Difference) distribution of the 5-min. volume/speed estimation results for one morning and one afternoon period, and Tables 5 and 6 show the Mean Error (MPD & MAE) of each test site for four days. As indicated in these figures and tables, the model showed very satisfactory performance with the morning data set, where traffic was relatively uncongested, while the estimation error increased in the two afternoon peak periods, in which traffic was heavily congested due to inclimate weather conditions. For example, the comparisons for the Nov.7, 1989 morning data suggest that, out of 576 data points estimated by KRONOS (16 stations * 36 (5-min. time intervals)), 92% of volume and 82% of speed estimation results were within 15% of the actual measurements. However, during the afternoon of Nov. 20 peak period, only 62 % of volumes and 51 % of speeds were within 15 % of the actual measured data. Further, the MPD of volume for 2 mornings ranges from 0.6 % to 15.9 %, while the speed MPD for the same 2 mornings was between 2.5 % and 28.0 %. For two afternoons, the volume estimation MPD ranges from 7.1 % to 27.6 % and the speed MPD between 2.8 % and 31.7 %. The higher error in speed estimation indicates the need to use multiple speed-density relationships reflecting weather conditions rather than a single curve throughout. Further, the speed estimation error indicates the need for more effort in calibrating speed-density curves and estimating the capacities. The latter is a very important issue common to all macroscopic simulation models and is currently being investigated. Overall, the test results using four peak periods show very satisfactory performance of the enhanced KRONOS program in light to moderate traffic conditons, while they indicate further investigation to explain the higher differences during heavy congestion. One possible explanation is the lack of sufficient stable data for deriving the speed-density relationship during such conditions. Clearly either a new methodology for this has to be developed or more advanced state equations have to be developed that do not require employment of such relationships.

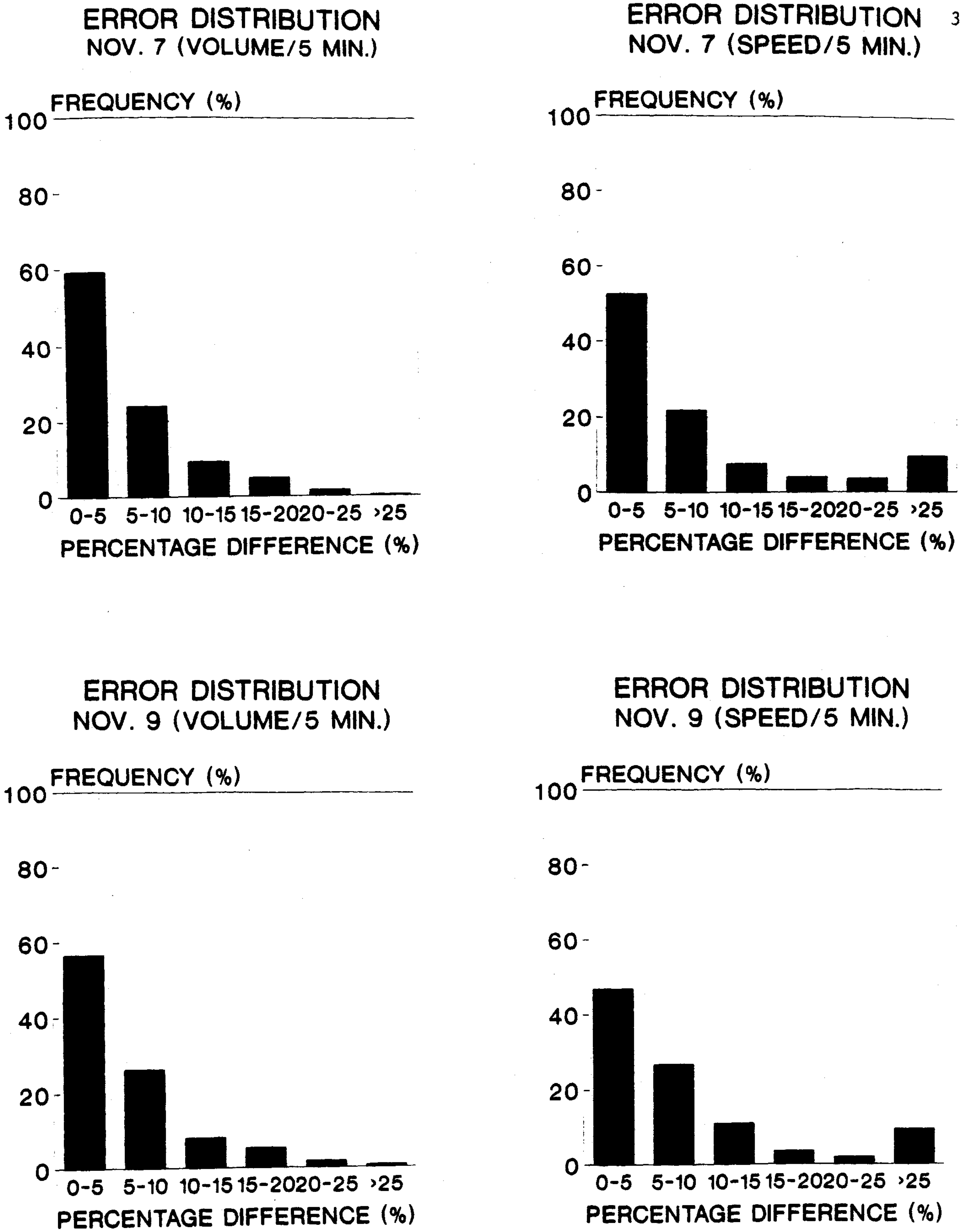

Fig. 15 Error distribution (Morning traffic)

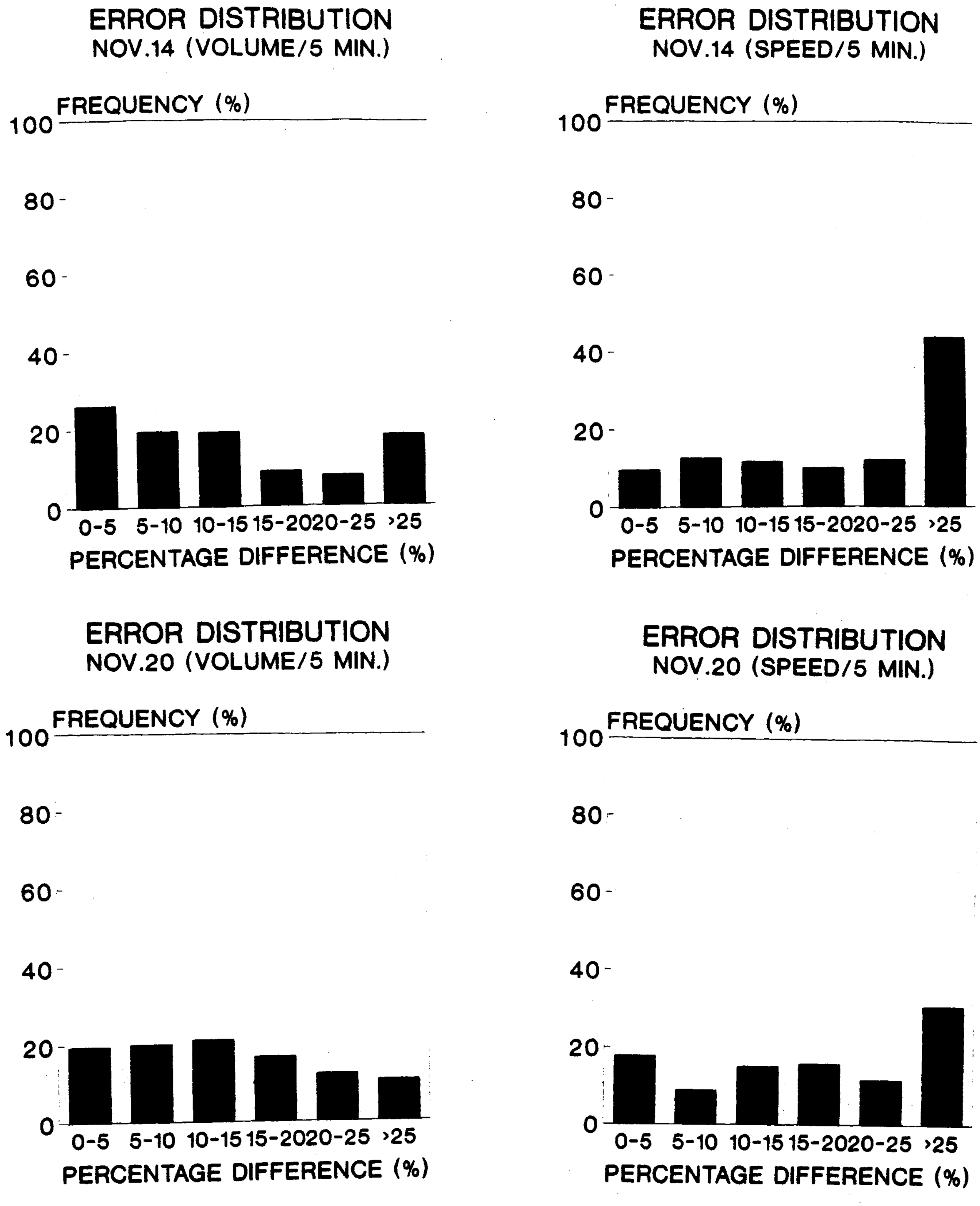

Fig. 16 Error distribution (Afternoon traffic)

Table 5 Mean Error of the Volume/Speed Estimation Results (Morning)

(6:00 - 9:00 a.m.)

Site	Nov. 7				Nov. 9			
	Volume/5-min.		Speed/5-min.		Volume/5-min.		Speed/5-min.	
	MPD	MAE*	MPD	MAE**	MPD	MAE	MPD	MAE
86N	0.7	13.6	4.6	2.3	0.6	12.3	6.9	3.8
82N	2.5	42.6	3.3	1.9	2.3	41.9	3.8	1.9
78N	6.6	96.6	7.8	3.7	7.8	116.8	5.6	3.2
76N	4.0	57.3	3.7	2.5	4.4	64.6	4.8	2.5
73N	3.5	54.3	N/A	N/A	5.0	79.1	6.1	3.4
70N	3.5	53.7	3.3	1.9	4.5	72.8	4.2	2.4
66N	4.7	65.2	2.5	1.4	5.9	82.9	4.5	2.3
63N	14.4	196.0	5.9	2.4	15.9	221.5	16.4	5.1
62N	8.4	133.7	N/A	N/A	9.6	155.1	N/A	N/A
61N	6.9	139.8	24.2	10.5	5.9	125.3	28.0	13.3
60N	7.1	128.0	21.8	10.5	6.9	129.7	17.3	7.3
55N	4.6	88.2	15.4	8.2	3.9	77.4	16.5	6.8
53N	7.1	134.2	20.5	9.3	6.5	127.1	26.1	9.8
46N	4.9	95.7	7.9	4.3	4.1	82.1	6.1	2.4
42N	4.8	73.8	4.4	2.6	3.4	65.0	4.0	2.4
35N	4.2	73.3	3.8	2.1	3.6	67.8	4.9	2.7

*: veh/hr/lane ** : miles/hr

Table 6 Mean Error of the Volume/Speed Estimation Results (Afternoon)

(3:30 - 6:30 p.m.)

Site	Nov. 14				Nov. 20			
	Volume/5-min.		Speed/5-min.		Volume/5-min.		Speed/5-min.	
	MPD	MAE*	MPD	MAE**	MPD	MAE	MPD	MAE
46S	5.5	83.0	27.0	8.6	13.1	223.9	26.2	11.5
50S	7.1	114.5	27.1	9.8	14.4	255.7	31.6	11.1
53S	10.2	156.1	N/A	N/A	11.5	198.1	30.3	11.5
60S	9.2	137.3	31.4	7.1	20.8	359.2	30.8	6.0
61S	13.9	211.8	21.8	6.6	15.7	276.7	31.7	8.3
62S	10.4	145.2	20.7	8.7	8.2	131.8	2.8	1.3
63S	27.6	273.6	30.2	12.4	20.0	238.5	15.6	7.1
70S	16.1	217.8	13.6	7.3	8.4	141.3	20.0	11.2
76S	17.1	215.4	14.6	7.5	7.9	123.3	16.4	9.4
78S	24.1	246.2	N/A	N/A	17.1	224.7	7.1	3.2

*: veh/hr/lane   ** : miles/hr

V. SENSITIVITY ANALYSIS

V.1 Overview of the sensitivity analysis

In this chapter, the sensitivity of the KRONOS simulation models with respect to the changes in the input parameters, i.e., the speed-density relationship and capacities of each individual freeway segment, is investigated. While the current KRONOS program uses a single speed-density relationship for the entire freeway section to be simulated, the capacities of individual segments can be provided by the user. Using these capacities for each segment, KRONOS adjusts the default or user-specified speed-flow-density relationship to reflect specific traffic conditions of each segment. Fig.17 illustrates the effects of different capacities on the flow-density relationships and the corresponding speed-density relationships. In this project, the effects of the variations in capacities, and thus, the effects of different speed-flow-density relationships on the simulation results are investigated for major types of freeway segments, i.e., merging, diverging and weaving segments.

V.2 Merging segment

Figures 18 and 19 show the geometrics of the merging area and the demand pattern used in this sensitivity analysis. Four types of upstream arrival demand were used; Light-uncongested (volume/capacity : 35-45%), high-uncongested (v/c: 75-85%), high-congested (v/c: 75-85%), heavy-congested (v/c: 35-45%) demand patterns. For each demand pattern the example merging area was simulated for a 30-min. period with 3 different values of capacity in the merging area (zone 2) -- 5280, 5860, and 6440 vehicles per hour -- while the capacities of other zones, i.e., zone 1 and zone 3, remained constant.

Table 7 shows the percentage change in volume and speed for each zone for the 30-min. period. For each demand pattern, the case with the lowest capacity

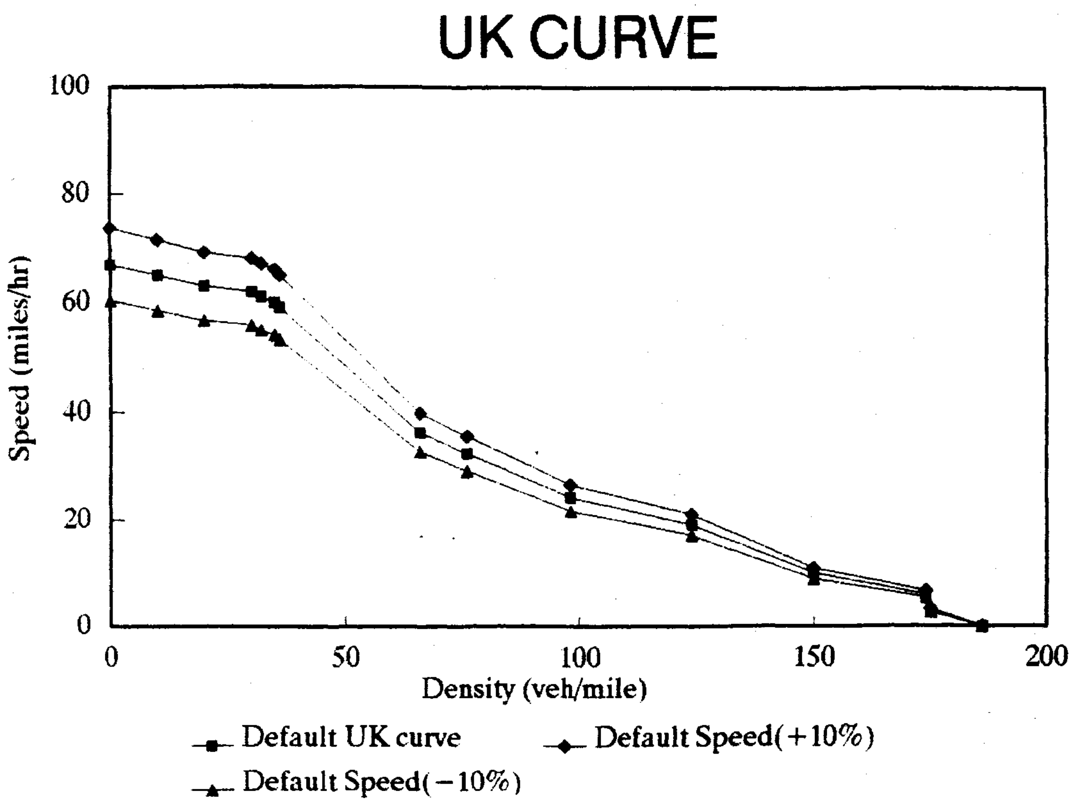

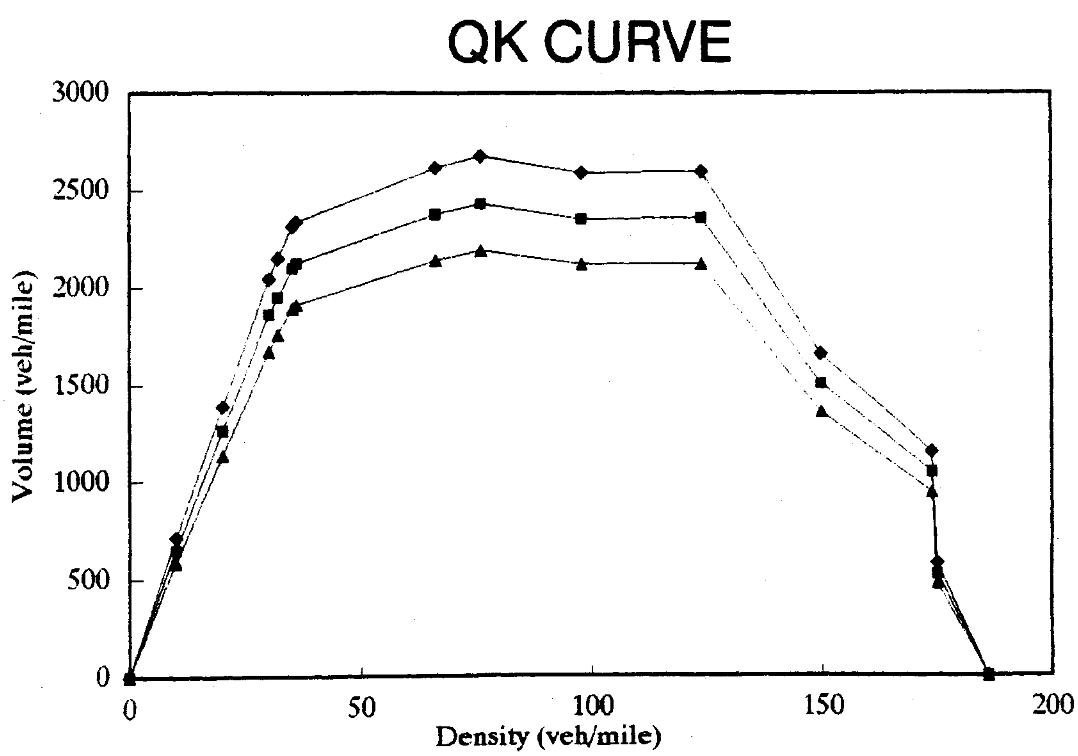

Fig. 17 Adjustments of speed(flow)-density relationship

fi

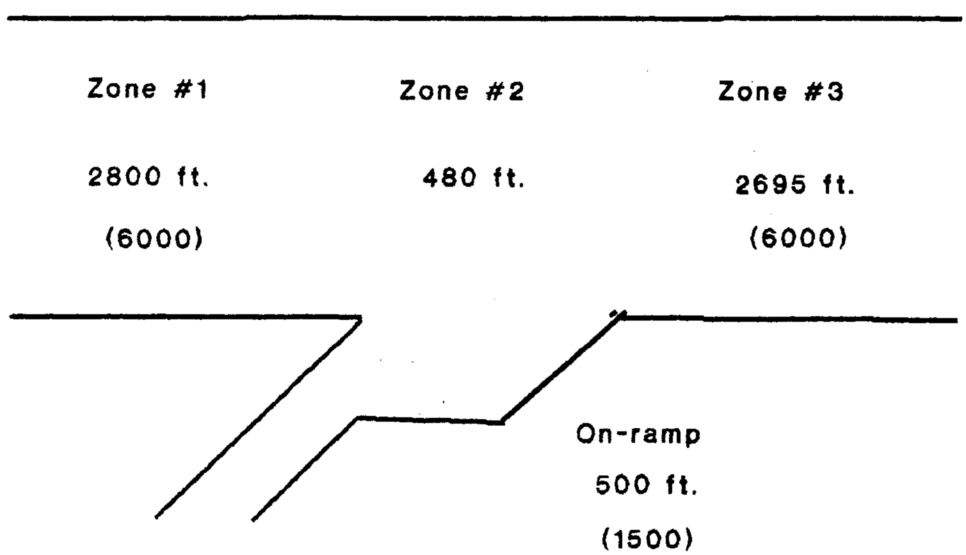

() capacity in veh/hr.

Capacity of Zone #2:

Base Case - 5220 vph

Case 2 - 5800 vph

Case 3 - 6380 vph

Fig. 18 Sample merging area

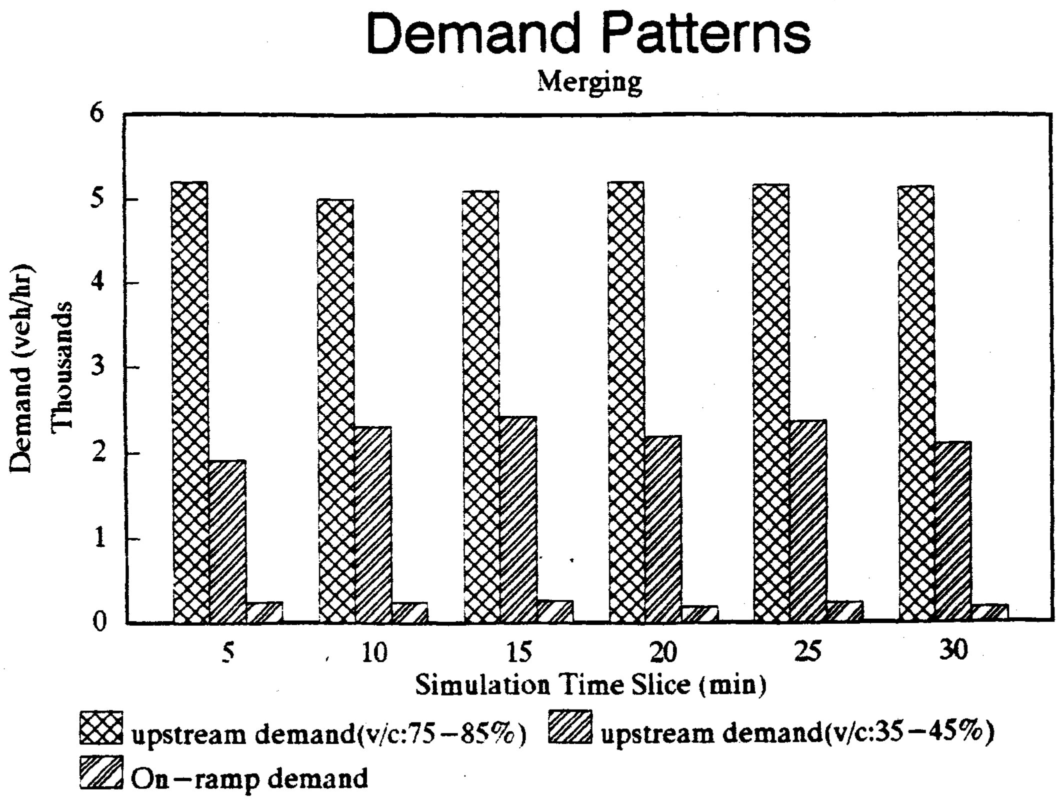

Fig. 19 Demand pattern for the sample merging area

Table 7. Sensitivity of the merging model

Capacity increase in Zone#2	Upstream Arrival Demand	Flow Type	Volume changes in (%) Zone #1	Zone #2	Zone #3	Speed changes in (%) Zone #1	Zone #2	Zone #3
+11%	V/C:35-45 (%)	Uncong.	0.00	1.31	-0.35	0.00	11.65	0.00
		Cong.	0.04	3.80	0.00	-0.64	0.96	0.00
	V/C:75-85 (%)	Uncong.	0.17	5.32	-0.50	0.17	20.70	0.61
		Cong.	0.25	9.77	0.68	0.46	0.12	-10.39
+22%	V/C:35-45 (%)	Uncong.	0.00	1.91	-0.61	0.00	23.38	0.00
		Cong.	0.06	6.65	0.00	0.00	2.24	0.00
	V/C:75-85 (%)	Uncong.	0.00	8.48	-0.93	0.17	41.57	1.01
		Cong.	0.17	12.06	-0.89	0.23	-2.66	-11.31

(5280 vph) was used as the base case. As illustrated in Table 7, for the uncongested traffic, the capacity increase in the merging segment resulted in a substantial increase in speed while the volume increase was relatively insignificant. In the case of congested traffic, the volume increase proved to be more significant than the speed increase. Further, in the case of the congested-high demand (V/C: 75-85%), an 11% increase of capacity resulted in an approximately 10% increase in volume, while an additional 11% increase in capacity resulted in only an additional 3% increase in volume. This appears to indicate that as the capacity approaches the point at which conditions would become uncongested, the incremental increase in volume approaches zero.

V.3 Diverging segment

Figures 20 and 21 show the geometrics of the diverging area and the demand pattern used in this sensitivity analysis. Four types of upstream arrival demand were used; Light-uncongested (volume/capacity : 35-45%), high-uncongested (v/c: 75-85%), high-congested (v/c: 75-85%), heavy-congested (v/c: 35-45%) demand patterns. For each demand pattern the example diverging area was simulated for a 30-min. period with 3 different values of capacity in the diverging area (zone 2) -- 5220, 5800, and 6380 vehicles per hour -- while the capacities of other zones, i.e., zone 1 and zone 3, remained constant.

Table 8 shows the percentage change in volume and speed for each zone for the 30-min. period. For each demand pattern, the case with the lowest capacity (5220 vph) was used as the base case. As illustrated in Table 8, for the uncongested traffic, the capacity increase in the merging segment resulted in a substantial increase in speed while the volume increase was much smaller. In the case of congested traffic, the volume increase proved to be more significant than the speed increase. Further, in the case of the congested-high demand (V/C: 75-85%), an 11% increase of capacity resulted in an approximately 11%

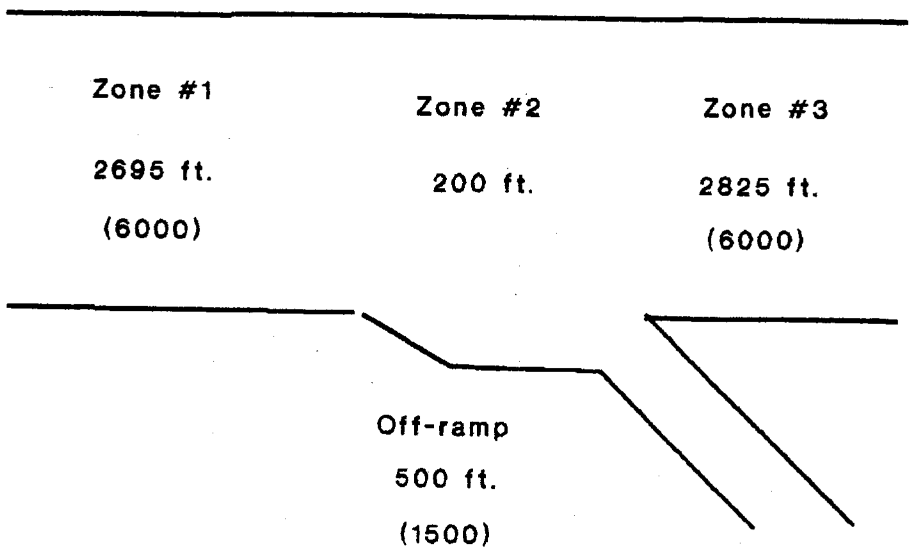

() capacity in veh/hr

Capacity of Zone #2:

Base case - 5400 vph

Case 2 - 6000 vph

Case 3 - 6600 vph

Fig. 20 Example diverging area

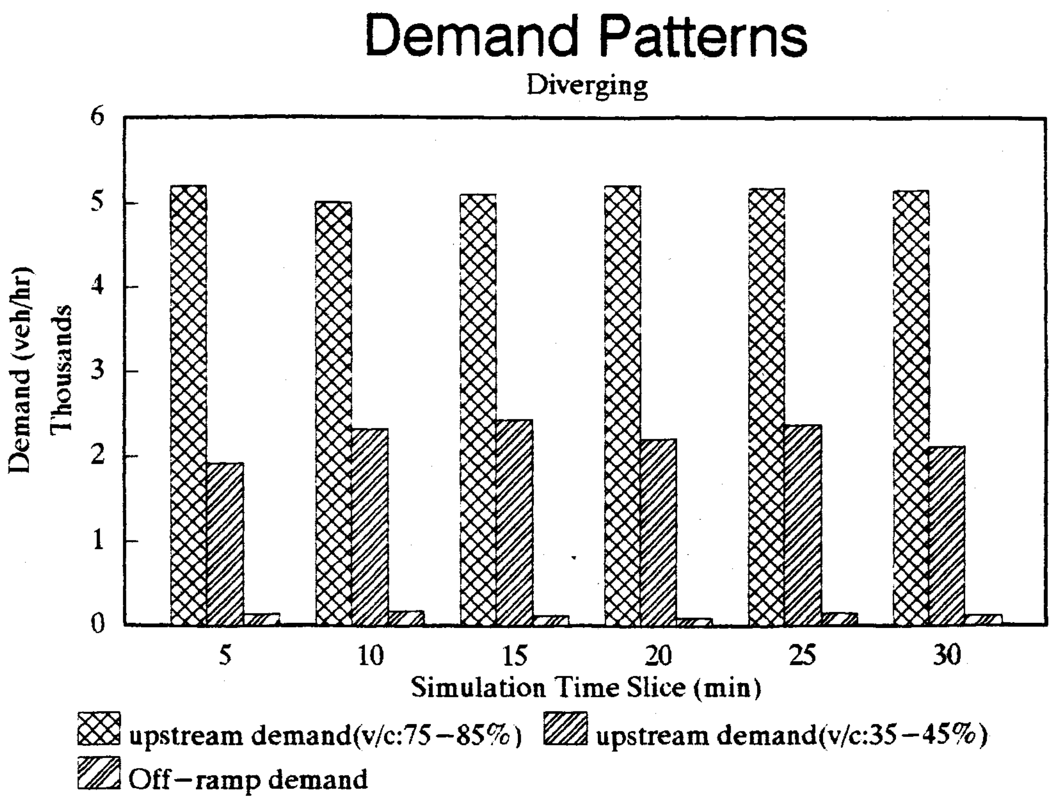

Fig. 21 Demand pattern for the example diverging area

Table 8 Sensitivity of the diverging model

Capacity increase in Zone#2	Upstream Arrival Demand	Flow Type	Volume changes in (%)			Speed changes in (%)		
			Zone #1	Zone #2	Zone #3	Zone #1	Zone #2	Zone #3
+11%	V/C:35-45 (%)	Uncong.	0.00	6.42	-0.50	0.00	11.31	0.00
		Cong.	0.03	4.75	0.00	0.00	2.78	0.00
	V/C:75-85 (%)	Uncong.	-0.01	3.70	-0.02	0.00	16.93	0.07
		Cong.	0.09	11.40	0.34	1.87	8.08	-4.93
+22%	V/C:35-45 (%)	Uncong.	0.00	12.28	-1.16	0.00	22.70	0.00
		Cong.	0.07	10.45	0.00	0.00	5.84	0.00
	V/C:75-85 (%)	Uncong.	-0.01	9.99	-0.03	0.00	29.63	0.07
		Cong.	0.12	22.71	0.16	3.26	14.00	-9.63

increase in volume, while an additional 11% increase in capacity also resulted in only an additional 11% increase in volume. This result fulfilled expectations, since for a congested situation in a diverging zone, the factor limiting the volume is the capacity of that zone. For speeds, the change was not as regular. However, across both tested levels of congestion (congested and uncongested) and both volume-to-capacity ratio levels, there is a tendency illustrated in Table 8 of speeds to increase at a slower rate for the second incremental difference in capacity than it did for the first incremental difference in capacity.

V.4 Weaving segment

Figures 22 and 23 show the geometrics of the weaving area and the demand pattern used in this sensitivity analysis. Four types of upstream arrival demand were used; Light-uncongested (volume/capacity : 35-45%), high-uncongested (v/c: 75-85%), high-congested (v/c: 75-85%), heavy-congested (v/c: 35-45%) demand patterns. For each demand pattern the example weaving area was simulated for a 30-min. period with 3 different values of capacity in the weaving area (zone 2) -- 3600, 4000, and 4400 vehicles per hour -- while the capacities of other zones, i.e., zone 1 and zone 3, remained constant.

Table 9 shows the percentage change in volume and speed for each zone for the 30-min. period. For each demand pattern, the case with the lowest capacity (3600 vph) was used as the base case.

As illustrated in Table 9, for uncongested traffic, the capacity increase in the merging segment resulted in a substantial increase in speed -- on the order of 10 to 20 percent (depending on the volume-to capacity ratio) for each 11 percent increase in capacity -- while the volume increase was much less significant -- a maximum of 5 percent for each 11 percent increase in capacity. In addition, for the lower values of volume-to-capacity ratio, the percentage

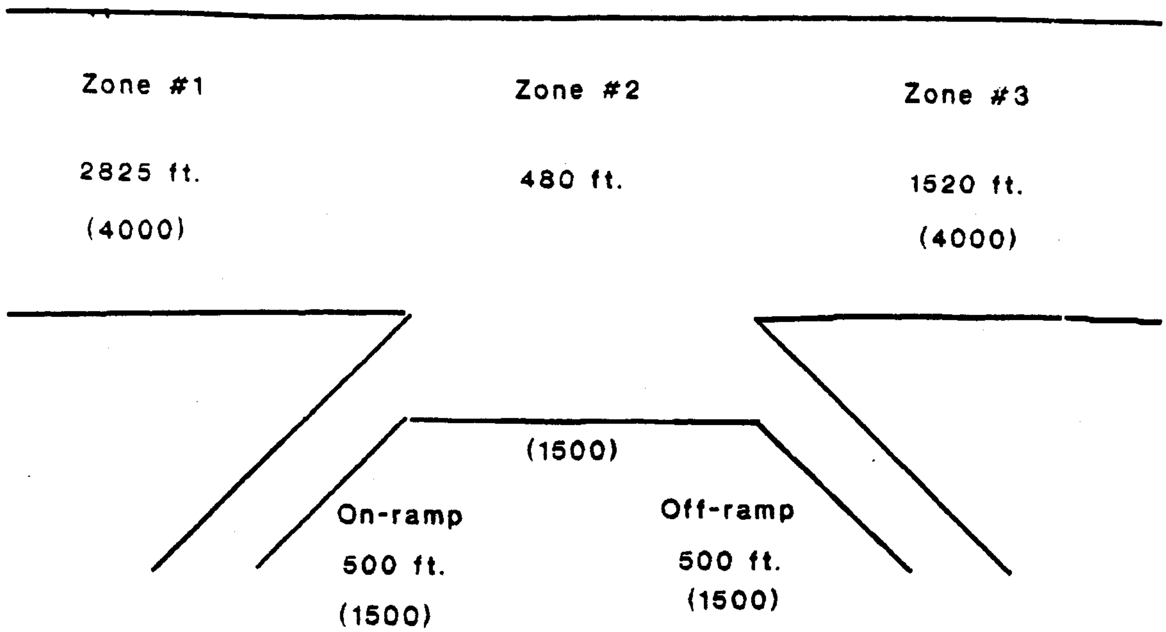

() capacity in veh/hr.

Capacity of Zone #2

Base Case - 3600 vph

Case 2 - 4000 vph

Case 3 - 4400 vph.

Fig. 22 Geometrics of the example weaving area

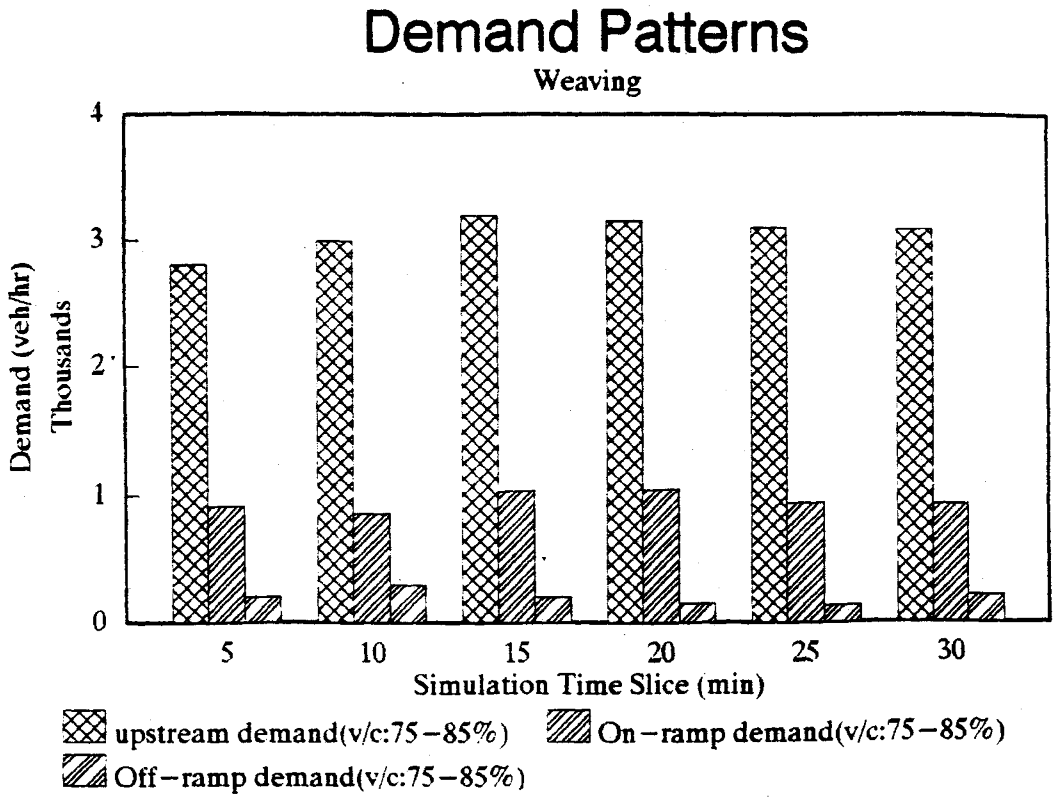

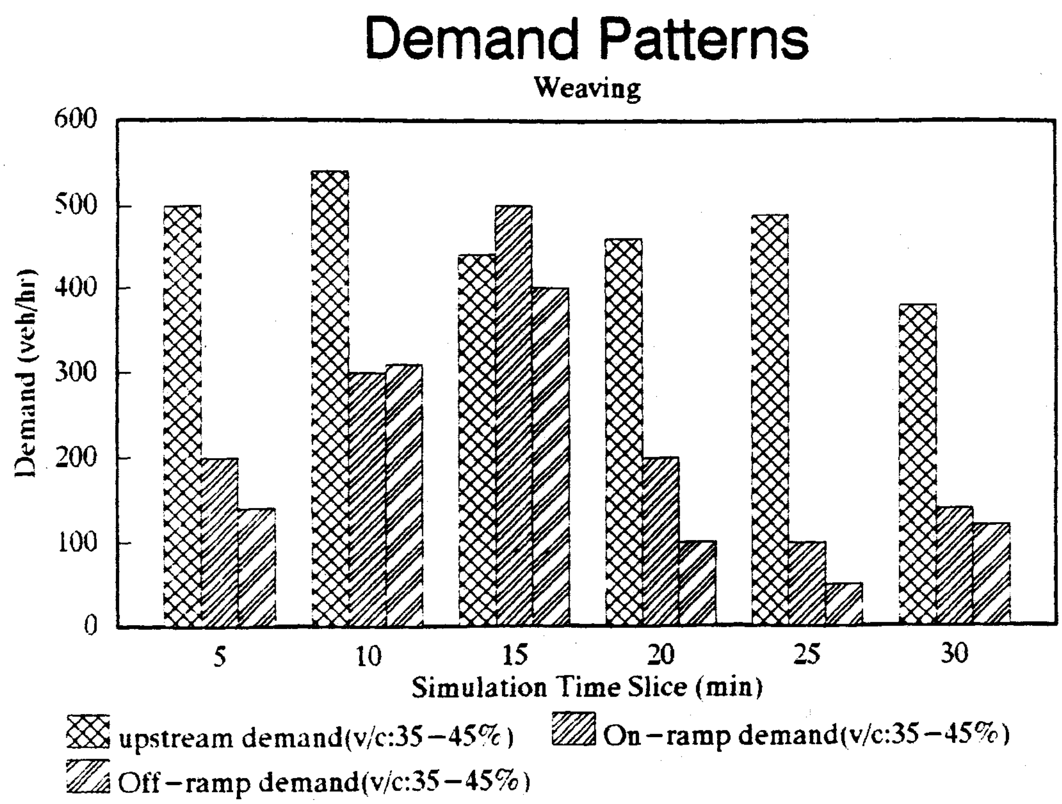

Fig. 23 Demand pattern of the example weaving area

Table 9 Sensitivity of the weaving model

Capacity increase in Zone#2	Upstream Arrival Demand	Flow Type	Volume changes in (%) Zone #1	Zone #2	Zone #3	Speed changes in (%) Zone #1	Zone #2	Zone #3
+11%	V/C:35-45 (%)	Uncong.	0.00	5.02	2.58	0.00	10.34	0.00
		Cong.	-0.26	1.85	0.00	0.15	3.41	0.00
	V/C:75-85 (%)	Uncong.	0.00	3.98	0.04	0.00	20.37	-0.06
		Cong.	-0.57	4.97	-0.64	-0.86	2.04	-0.86
+22%	V/C:35-45 (%)	Uncong.	.0.00	6.84	2.58	0.00	22.49	0.00
		Cong.	-0.14	3.44	0.00	0.15	4.60	0.00
	V/C:75-85 (%)	Uncong.	0.00	5.48	0.08	0.00	39.56	0.00
		Cong.	-1.51	8.41	-2.40	-1.27	3.21	-3.45

increase in volume was higher and in speed was lower than for the higher values of volume-to-capacity ratio.

In the case of congested traffic, the percentage increases in both volume and speed were, in general, smaller than in the uncongested case for the same incremental increases in capacity. For an incremental increase of 11% in capacity, the highest percentage change in either volume or speed was less than 5 percent. In addition, for both speed and volume, the table revealed a tendency for the percentage increase in the measure to be greater for the first incremental capacity increase than for the second incremental increase.

In general, the sensitivity analyses performed indicate that volumes are more sensitive to changes in capacity in congested situations and in situations where the volume is relatively close to capacity. Volumes are less sensitive to changes in capacity in relatively uncongested conditions. Conversely, speeds appear to be more sensitive to incremental changes in capacity in relatively uncongested conditions. This finding was somewhat surprising, since absolute speeds in uncongested conditions are higher than for congested conditions and, consequently, a greater change in absolute speed is required to attain the same percentage change as for the congested case. Yet the higher percentage changes are consistently seen in the tables for the uncongested simulations.

VI. CONCLUSIONS AND FURTHER RESEARCH NEEDS

The enhanced KRONOS program provides a practical tool to traffic engineers for evaluating various freeway design and management alternatives, including decisions frequently made in freeway operations, such as ramp metering, lane blockages, construction and maintenance operations and others. The program, taking advantage of the recent advancements in the microcomputer hardware technology, has the user-friendly menu-driven input/output modules which significantly reduced the time-consuming effort to prepare input and analyze the results. The test results with the field data collected from an 8-mile section of the I-35W freeway show very promising model performance in estimating volume and speed through time.

While the data used in this study provide sufficient information to evaluate the overall performance of the model, more detailed measurements of speed, density and volume at shorter time and space increments are required to develop accurate models that can be applicable in a real-time environment. Future plans include the collection of such detailed data using the video-detection system currently being developed at the University of Minnesota. A total of 38 video-detectors are planned to be installed by 1993 along a 2.5-mile section of the I-394 freeway in Minneapolis, Minnesota (9). This section will serve as a live laboratory for collecting and studying traffic characteristics as well as for testing and validating the KRONOS program in a more rigorous fashion by fully analyzing the traffic dynamics in merging, diverging and weaving areas. Further enhancements to KRONOS needed to be made include optimal calibration of multiple speed-density relaitonships for each section of freeway, High Occupancy Vehicle (HOV) priority treatment, corridor modelling with demand-diversion, estimation of optimal ramp metering rates, and development of high-order continuum models which do not require equilibrium speed-density relationships, etc. Finally an input interface which can automatically extract the necessary input information (geometric and demand) from available databases will be developed, so that time-consuming manual efforts in preparing the input data can be.minimized.

REFERENCES

1. May A., Freeway simulation models revisited. Trans. Res. Rec. 1132, pp. 94-99, 1988.

2. Imada, T., May, A.D. FREQ8PE: A freeway corridor simulation and ramp metering optimizing model. Report UCB-ITS-RR-85-10. University of California, Berkley, 1985.

3. Payne, H.J. FREFLO: A Macroscopic simulation model of freeway traffic, Transp. Res. Rec. 772, pp. 68-75, 1979.

4. Wicks, D.A., Lieberman, E.B. Development and testing of INTRAS, a microscopic freeway simulation program. FHWA-RD-76-75.

5. Van Aerde, M., Voss, J., Ugge, A., and Case, E.R., Managing traffic congestion in combined freeway and traffic signal networks. ITE journal, Vol. 59, No.2, pp. 36-42, February 1989.

6. Rathi, A.K., Nemeth, Z.A., Freesim: A microscopic simulation model of freeway lane closures. Trans. Res. Rec. 1091, pp. 21-24, 1986.

7. Kwon,E., Lee, C.F., Kang, J., et al. Traffic management strategies for freeway corridors Phase II extension. Final report prepared for the Minnesota Department of Transportation, 1990.

8. Hall, F., Perasud, B., Evaluation of speed estimates made with single -detector data from freeway traffic management systems. Trans. Res. Rec. 1232, pp. 9 - 16, 1989.

9. Michalopoulos, P.G., Wolf, B., and Benke, R. Testing and field implementation of the Minnesota Video Detection System, In press, Transp. Res. Rec. 1990.